Main Manuscript for

Toxin resistance mechanisms span biological scales in the Royal Ground Snake *Erythrolamprus reginae*

Valeria Ramírez-Castañeda[1]*, Samantha A. Nixon [2], Dario Alarcón-Naforo[3], Fayal Abderemane-Ali[4], Richard W. Fitch[5], David Salazar-Valenzuela[6,7], Daniel L. Minor, Jr.[2,8,9,10,11], Rebecca D. Tarvin[1]*

[1]Museum of Vertebrate Zoology and Department of Integrative Biology, University of California, Berkeley, CA, 94720, USA

[2]Cardiovascular Research Institute, University of California, San Francisco, CA, 94158

[3]Departamento de Biología, Facultad de Ciencias, Universidad Nacional de Colombia, Bogotá, Colombia

[4]Department of Physiology, David Geffen School of Medicine, University of California, Los Angeles, CA, 90095, USA

[5]Department of Chemistry and Physics, Indiana State University, Terre Haute, IN, 47809, USA

[6]Centro de Investigación de la Biodiversidad y Cambio Climático (BioCamb) e Ingeniería en Biodiversidad y Recursos Genéticos, Facultad de Ciencias de Medio Ambiente, Universidad Tecnológica Indoamérica, Av. Machala y Sabanilla, Quito, Ecuador

[7]Laboratorio de Venómica y Toxinología Aplicada, Facultad de Ciencias de la Vida, Universidad Regional Amazónica Ikiam, Tena, Napo, Ecuador.

[8]Departments of Biochemistry & Biophysics, and Cellular & Molecular Biology, University of California, San Francisco

[9]California Institute for Quantitative Biomedical Research, University of California, San Francisco

[10]Kavli Institute for Fundamental Neuroscience, University of California, San Francisco

[11]Molecular Biophysics and Integrated Bio-imaging Division, Lawrence Berkeley National Laboratory, Berkeley, CA

* Valeria Ramírez-Castañeda, Rebecca D. Tarvin

Email: vramcas@stanford.edu, rdtarvin@berkeley.edu

This PDF file includes:

Main Text
Tables 1 to 5

Abstract

All predators of poisonous prey deal with toxins, yet we often lack an understanding of how the predators integrate various physiological adaptations to toxins. Here we investigate multiple complementary toxin resistance mechanisms in the pan-Amazonian snake *Erythrolamprus reginae* (Squamata: Colubridae), which consumes multiple species of poisonous frogs. We find that the toxin resistance mechanisms employed by *E. reginae* integrate novel behaviors, mutations in gene families, and plasticity in organ systems that help dampen possible costs of toxin exposure. Specifically, *E. reginae* exhibited longer handling times and aversion toward the poison frog *Ameerega trivittata*, demonstrating additional foraging costs and bringing into question prior assumptions about the species' propensity to consume toxic prey. In the liver, upregulation of transporters likely helps clear toxins following *A. trivittata* ingestion; additionally, protein extracts from the liver partially restored the activity inhibited by various small molecule toxins, including some toxins from *A. trivittata* and, unexpectedly, by neosaxitoxin, a guanidinium neurotoxin not known in the snake's diet. Further, mutations in the *E. reginae* voltage-gated sodium channel $Na_V1.4$ provide resistance to guanidinium toxins including TTX, STX, neoSTX. These findings indicate that a chemically diverse prey community can drive multi-scale evolutionary responses, with distinct mechanisms acting on distinct toxin classes and, in some cases, complementary mechanisms converging on the same compound. Together our results demonstrate a comprehensive assessment of toxin resistance, establishing that resistance to toxic prey necessitates adaptations across biological scales, and providing a roadmap for future studies of toxin resistance in emerging model species.

Main Text

Introduction

Predators deal with toxins in three major ways: 1) behavioral aversion, 2) metabolic detoxification, and 3) alternative or resistant molecular targets (Tarvin et al. 2023). The pressure to adapt to toxic prey tends to strongly impact the trophic structure of an ecosystem because many toxin resistance mechanisms exert trade-offs (e.g., in energy or access to resources) (Ferrer and Zimmer 2012; Scesa et al. 2024). Thus, the presence, absence, and comprehensiveness of toxin resistance shapes how organisms interact with toxic food sources. Predators of amphibians, for example, have to counteract multiple chemicals secreted from different species or individuals (J. W. Daly 1995; Daly 1998; Saporito et al. 2011). As a result, some predators avoid toxic prey (Skelhorn et al. 2016). However, others have evolved to resist toxins through behavioral, physiological, or molecular adaptations. While some resistance mechanisms have been characterized, in general there has been a lack of comprehensive assessment across biological scales in a single organism (Tarvin et al. 2023). A complete understanding of toxin resistance requires an integrative approach assessing adaptations in behavior, detoxification, and molecular target binding sites within each species.

The pan-amazonian Royal Ground Snake *Erythrolamprus reginae* (Squamata: Colubridae) is a generalist predator that consumes multiple species of poisonous frogs that have a diverse set of steroidal and alkaloid defenses (Albarelli and Santos-Costa 2010; Pašukonis and Loretto 2020). *E. reginae* harbors substitutions in voltage-gated sodium (Na_V) channels that putatively provide target-site resistance (TSR) to two guanidinium toxins: tetrodotoxin (TTX), which is present in some bufonids, and saxitoxin (STX), for which a local source is unknown (Ramírez-Castañeda et al. 2026). Other types of resistance mechanisms, such as metabolic detoxification and behavioral aversion, are uncharacterized. More generally, the resistance mechanisms for the vast majority of naturally occurring toxins, including most dendrobatid toxins, remain unknown, especially in predators such as snakes that are both elusive and scarce. We investigated toxin resistance mechanisms in *E. reginae* including putative TSR sites, and also other mechanisms such as upregulation of xenobiotic enzymes and/or toxin-binding proteins.

We aimed to systematically evaluate the presence of toxin resistance in *E. reginae.* First, we characterised the feeding preference of *E. reginae* for highly poisonous versus non-toxic frog prey. Second, we validated the impact of previously identified mutations that are hypothesized to provide target-site resistance (TSR).

Considering that snake channels were only resistant to guanidine toxins and not to other frog toxins, we thirdly investigated the mechanisms of metabolic detoxification in several organs. Our findings offer a compelling and comprehensive example of how predators adapt to diverse toxic pressures, revealing the physiological and evolutionary complexity of toxin resistance.

Results

Behavioral Aversion

First, we aimed to establish the ecological relevance of toxin resistance mechanisms in *E. reginae* by offering a set of locally co-occurring frog prey with diverse chemical defenses and toxicity levels to fasted adult *E. reginae* snakes from Leticia, Amazonas, Colombia (Data S6). One highly toxic frog included was the dendrobatid *Ameerega trivittata*, which secretes histrionicotoxins (HTX), pumiliotoxins (PTX), and decahydroquinolines (DHQ) (Daly 2005; Santos et al. 2016), and is a known prey item of *E. reginae* (Pašukonis and Loretto 2020). The other frogs included putatively non-toxic hylid species, primarily *Scinax ruber*, as well as *Dendropsophus* sp. and *Sphaenorhynchus lacteus*. Additionally, some snakes were offered mildly toxic frogs, *Leptodactylus* sp. and *Rhinella margaritifera*, which secrete amines and steroidal toxins (respectively) (Cei et al. 1967; Daly et al. 1987; Prates et al. 2012). Chemical analysis using gas chromatography mass spectrometry (GC-MS) confirmed the presence of multiple neurotoxic alkaloids from whole skins of *A. trivittata* ($n = 6$), including DHQs, N-methyl-DHQs, 5,8-indolizidines, and HTXs, but not from whole skins of *S. ruber* ($n = 6$).

Only 4 of 10 *E. reginae* snakes consumed *A. trivittata* when offered. One died after ingestion (Fig. 1A-B, Data S1-S2). If the snake did not consume *A. trivittata* within two hours, we removed the *A. trivittata* and offered another prey option (*S. ruber*, *Dendropsophus* sp., *Sphaenorhynchus lacteus*, *Leptodactylus* sp., or *R. margaritifera*). In the 6 cases where snakes refused the *A. trivittata* prey, they showed no interest in feeding and in general did not seem to treat the frog as possible prey. All 6 of the snakes that refused *A. trivittata* consumed the second prey offered, usually within one minute.

Snakes showed significant differences in the handling and consumption of *A. trivittata* versus other prey, taking longer to swallow them (Fig. 1C) and exhibiting a unique "dragging" behavior—rubbing the frog along the ground (see video Data S2 and YouTube (https://www.youtube.com/shorts/CUsNjgG3jTA)). This behavior was exclusively observed during *A. trivittata* ingestion (Fig. 1D).

Validation of TSR to Guanidinium Toxins

Putative TSR has been previously identified in Na_V sequences of *Erythrolamprus* snakes (Feldman et al. 2012; Ramírez-Castañeda et al. 2026). In some *E. reginae* populations, Na_V channels exhibit amino acid substitutions at sites experimentally reported to confer tetrodotoxin (TTX) resistance in $Na_V1.1$, $Na_V1.3$, $Na_V1.4$, $Na_V1.6$, and $Na_V1.8$ (Terlau et al. 1991; Geffeney et al. 2005; Vaelli et al. 2020; Ramírez-Castañeda et al. 2026). However, physiological experiments are necessary to confirm whether amino acid substitutions actually alter toxin sensitivity or affect protein function (Abderemane-Ali et al. 2021). We tested the hypothesis that putative TSR-associated substitutions in *E. reginae* $Na_V1.4$ reduce channel sensitivity to guanidinium neurotoxins. To do so, we synthesized and examined two variants: a putative resistant variant (*Er*$Na_V1.4$-R) found in *E. reginae* snakes in Leticia, Amazonas, Colombia, which harbors five amino acid substitutions at functionally relevant sites (Fig. S1), and a non-resistant variant (*Er*$Na_V1.4$-NR) from the same population, which lacks these mutations, as described in (Ramírez-Castañeda et al. 2026) (Fig. S1, Data S4). Importantly, we synthesized the wild-type *E. reginae* $Na_V1.4$ channels rather than introducing point mutations into a model organism sequence, preserving natural channel variation and its full response to toxin exposure. The resulting experiments provide one of the few sets of electrophysiological data for a snake Na_V channel to date (McGlothlin et al. 2014).

To investigate the properties of *Er*$Na_V1.4$, we tested their toxin responses using two-electrode voltage-clamp (TEVC) recordings in *Xenopus laevis* oocytes, we compared the toxin responses of

ErNa_V1.4-R and *Er*Na_V1.4-NR, alongside the human Na_V1.4 (*Hs*Na_V1.4) channel as a control (Fig 2). We conducted concentration–response curves for each guanidinium toxin (Fig 2 A-B, E-G, I-K) and found that the IC_{50} values (Table S3) for *Er*Na_V1.4-R are extremely high, in some cases, even the highest toxin concentrations applied had negligible effect on channel activity, making a precise IC_{50} calculation impossible (Fig. 2D & 2H, *Er*Na_V1.4-R TTX & STX IC_{50} >> 3000 nM; neoSTX IC_{50} >> 333 nM; Fig 2L). In contrast, *Er*Na_V1.4-NR exhibited a sensitivity profile closely aligned with that of *Hs*Na_V1.4, with the following rank order: neoSTX > STX > TTX (Fig. 2D, 2H & 2L, IC_{50} 0.4048 nM ± 0.235 nM, 6.565 nM ± 1.013 nM, and 18.09 ± 2.02 nM, respectively). IC_{50} values for *Hs*Na_V1.4 are reported in Table S3. These results demonstrate that TSR in *Er*Na_V1.4-R confers high resistance to TTX, STX, and neoSTX in *E. reginae*.

To investigate whether the resistance mutations affected core channel properties, we tested whether these changes affected the voltage-dependence of activation and inactivation (Fig. S8; $Vactivation_{1/2}$ —*Er*Na_V1.4-R: -23.52 mV ± 3.554 mV; *Er*Na_V1.4-NR: -22.98 nV ± 3.382 mV; $VInactivation_{1/2}$ —*Er*Na_V1.4-R: -52.47 ± 2.929; *Er*Na_V1.4-NR: -53.32 ± 3.229) (Fig. S8 and Table S3). Inactivation and activation curves showed no differences, suggesting that the substitutions distinguishing the two variants do not affect inactivation, consistent with previous findings (del Carlo et al. 2024).

***Assessment of TSR to Lipophilic Alkaloids Found in* Ameerega trivittata**

Na_V1.4 has been identified as a target of several toxins secreted by *A. trivittata*, including HTX and PTX (Daly and Spande 1986; Vandendriessche et al. 2008; Santos et al. 2016). To test for TSR to these toxins, we repeated the above experiments with *A. trivittata* (toxic) and *S. ruber* skin secretions (non-toxic control) as well as isolated compounds found in *Ameerega* spp.: HTX **293A,** H_8-HTX, PTX **251D**, DHQ **167,** and DHQ **195A** (Fig 3 & Fig S7).

ErNa_V1.4-R did not exhibit resistance to *A. trivittata* skin secretions, which reduced the current by ~20% (Fig. 3C). As expected, the non-poisonous frog skin secretion did not reduce currents (*S. ruber*, Fig. 3F). Consistent with the skin secretion experiments, *Er*Na_V1.4-R did not exhibit resistance to PTX **251D** or H8-HTX but showed marginal resistant behavior over the low effect toxins HTX **293A**, DHQ **167** and DHQ **195A**. *Hs*Na_V1.4 did not show resistance to any of the isolated toxins, which caused current reductions of ~10%-60% (One-tailed t-test, $P \leq 0.01$; Fig. S7). These findings suggested that *E. reginae* relies on toxin resistance mechanisms other than TSR to consume *A. trivittata*.

Metabolic Detoxification

Given that we found limited evidence for TSR in the *E. reginae* muscle Na_V channel to *A. trivittata* defenses, we then conducted two experiments to test for the presence of metabolic detoxification mechanisms in response to both the guanidinium alkaloids and *A. trivittata* alkaloids. First, we applied a recently developed semi-automated planar patch-clamp electrophysiology assay (Zakrzewska et al. 2025) to screen liver tissue for toxin neutralization activity by measuring *Hs*Na_V1.4 currents sequentially elicited under saline (baseline), toxin, incubated toxin:liver extract, and liver extract (Fig. S3). We incubated toxins with *E. reginae* liver extract for 30 minutes at room temperature to allow any proteins to bind to or modify the toxins. Restoration of channel activity in the presence of the incubated toxin:liver extract, relative to baseline and toxin-alone block, was interpreted as evidence for detoxifying or toxin-binding proteins in the liver (Fig. 4). *E. reginae* liver extracts were compared against liver extracts from two control (toxin-sensitive) species: the house mouse (*Mus musculus*) and another snake, *Contia tenuis,* a North American colubrid with no known natural exposure to dendrobatid alkaloids. None of the tested liver extracts significantly inhibited *Hs*Na_V1.4 currents when applied alone (Fig. 4B, Fig. S4 and S5). Remarkably, preincubation of *E. reginae* liver extract ameliorated the effects of PTX **251D**, H8-HTX, and HTX **283A**, with the greatest current recovery for HTX **283A** (76.3 ± 9.1%, Fig. 4B). *E. reginae* liver also neutralized the effect of *A. trivittata* skin extract by 16.6 ± 2.7% (Fig. 4A) and of neoSTX by 61.1 ± 6.0% (Fig. 4F), but it had no impact on TTX or STX. Mouse liver extract did not restore sodium channel activity for any toxin (Fig. 4 and Fig. S4), indicating that amelioration of the toxin block was not driven by general

vertebrate liver detoxification enzymes. Similarly, *C. tenuis* liver extract had no effect on any dendrobatid toxin, STX, or TTX, but it completely ameliorated block by neoSTX (91.5 ± 7.4%) (Fig. 4F and Fig. S5).

Second, because toxin resistance can also be modulated by increased expression of specific genes involved in toxin breakdown, binding, and clearance (Tarvin et al. 2023), we generated transcriptomes from four digestive tissues (tongue, stomach, liver, and gut) in *E. reginae* that had consumed *A. trivittata* (n = 3), *Scinax ruber* (n = 3), or were fasting (n = 3) (Data S7). Expression profiles clustered primarily by tissue, with tongue being most distinct (Fig. S6A–B). The greatest number of upregulated genes was observed in response to *A. trivittata* consumption, with the liver showing the strongest transcriptional response among the tissues (Fig. 5A–B). Among the most upregulated genes were members of the solute carrier (SLC) family (Fig. S6C). In contrast, *S. ruber* elicited the weakest transcriptional activation. Fasting snakes showed upregulation of some genes, particularly in the stomach, likely related to canonical responses to starvation (Wei et al. 2025). Gene Ontology (GO) analyses revealed significant enrichment of membrane-bound proteins involved in transport activity (Fig. 5C) in *A. trivitatta*-fed snakes, but no enrichment of plasma proteins known to bind xenobiotics (Fig. S6D; Data S3) (Alvarez-Buylla et al. 2023).

Discussion

E. reginae snakes exhibit avoidance and specific behaviors when feeding on the toxic poison frog *Ameerega trivittata*

Toxic prey are traditionally considered a low-quality food because of the harmful effects of toxins (Marshall 1908; Speed 1993; Sherratt 2003; Sherratt et al. 2004; Halpin et al. 2013; Mappes et al. 2014; Skelhorn et al. 2016; Rowland et al. 2017), thus most predators avoid toxic prey. However, some predators have resistance mechanisms that allow them to take advantage of such resources. Most studies of predator behavior towards toxic prey focus on lab-trained predators or clay models (Darst and Cummings 2006; María Arenas et al. 2015; Halpin et al. 2020), and little is known about predator behavior in natural settings, especially in vertebrates. To bridge this gap, we conducted predation trials in the field with *E. reginae* and local frog prey. Despite published observations suggesting that *E. reginae* and other members of the genus readily consume toxic poison frogs (Myers et al. 1978; Feldman et al. 2012; Pašukonis and Loretto 2020), our findings demonstrate behavioral avoidance of *A. trivittata* by *E. reginae.* In addition, snakes displayed a unique dragging behavior and extended ingestion times in response to consuming *A. trivittata* that may help remove or break down some of the toxins; alternatively, such behavior may be a physiological consequence of exposure to *A. trivittata* toxins, some of which are neurotoxic (Anon 1986; Daly and Spande 1986). Thus, increased time and/or energy is expended by *E. reginae* when handling *A. trivittata.* Similar behaviors such as dragging, wiping, or washing have been reported in birds such as the hooded merganser (*Lophodytes cucullatus*), the southern ground hornbill (*Bucorvus leadbeateri*), and the grey heron (*Ardea cinerea*) when feeding on toxic/noxious frogs and newts (Hurlbert 1970; Kemp and Kemp 1978; Underhill 2015; Smith et al. 2024).

Behavioral avoidance and long feeding bouts underscore challenges posed by toxic prey at the organismal level. Optimal foraging theory predicts that predators may consume toxic prey when the alternative is less nutritious (Halpin et al. 2014; Santos et al. 2016) or more difficult to locate (Carle and Rowe 2014). However, multiple factors influence this type of foraging behavior, including physiological state: starved predators are more likely to consume toxic prey (Aubier and Sherratt 2020), and well-fed predators tend to make decisions based on prior experiences (Skelhorn and Rowe 2007). Therefore, profitability is not a binary variable but instead an integration of physiology, prey community, toxin resistance, and prior experience, and even when animals might possess some resistance to toxins, they may still endure substantial energetic and opportunity costs. We note that although they were not the focus of our feeding trials, *E. reginae* snakes showed no hesitation to consume toads (*R. margaritifera*), which contain bioactive steroids that some predators avoid (Mohammadi et al. 2016). Most colubrids are known to have genetic mutations that provide physiological tolerance to toad toxins (Ujvari et al. 2015; Mohammadi et al. 2016).

E. reginae $Na_V1.4$ has TSR to guanidinium but not poison frog alkaloids

We measured the sensitivity of the muscle-expressed $Na_V1.4$ sodium channel from *E. reginae* to the guanidinium alkaloids TTX, STX, and neoSTX, as well as to poison frog and hylid skin secretions, and to individual poison frog alkaloids. While TSR in the muscle-expressed $Na_V1.4$ sodium channel often underlies resistance to TTX and STX (Ramírez-Castañeda et al. 2026), the sensitivity of Na_V channels to poison frog alkaloids other than PTX **251D** and BTX has not been well studied (Vandendriessche et al. 2008; Wang and Wang 2017; Márquez et al. 2019; Abderemane-Ali et al. 2021; Alvarez-Buylla et al. 2022). To our knowledge, our study presents some of the first Na_V electrophysiological data for HTX **283A**, H8-HTX, DHQ **167**, and DHQ **195A**, and some of the first data for any snake Na_V channel (but see (McGlothlin et al. 2014)).

Er$Na_V1.4$-R was shown to be highly resistant to TTX, STX, and neoSTX (Fig. 2). Of the five amino acid substitutions present in *Er*$Na_V1.4$-R, D1539N and G1540D, which are located in the domain IV p-loop (selectivity filter), likely represent the primary contributors to the STX, neoSTX and TTX-resistant phenotype in *E. reginae,* as they were previously shown to confer high TTX and STX resistance in other organisms (Penzotti et al. 2001; Bricelj et al. 2005; Geffeney et al. 2005; McGlothlin et al. 2014; Vaelli et al. 2020). An additional substitution, P1550S, also occurs in this region and is found in dendrobatid frogs, though its functional role remains unclear (Tarvin et al. 2016). Structural modeling (Fig. 2M–P) shows that the remaining substitutions, I425L (domain I, segment 6) and S725N (domain II, segment 5), are located on the outer face of the pore domain, making it unlikely that they directly affect STX or TTX binding. Notably, S725N is also found in highly TTX-resistant species such as *Heterodon platirhinos* and *Thamnophis sirtalis* (Willow Creek population), despite not being previously identified as a TSR site (Feldman et al. 2016; Ramírez-Castañeda et al. 2026). Together, these data suggest that while five substitutions are present, resistance is most parsimoniously explained by the convergent D1539N and G1540D mutations in the domain IV p-loop.

The distribution of the D1539N and G1540D alleles in *E. reginae* $Na_V1.4$ has not been studied across the species' full geographic range, but the two alleles are found segregating in a single population in the Amazon basin (Leticia, Colombia). The same substitutions occur at homologous positions in *E. reginae* in $Na_V1.1$, $Na_V1.3$, $Na_V1.6$, and $Na_V1.8$ genes from the same gene family, as well as in multiple populations of another species of the same genus, *Erythrolamprus epinephelus* (Ramírez-Castañeda et al. 2026). TTX, STX, and neoSTX are common in some marine and terrestrial ecosystems but have not yet been documented in the known diet of *E. reginae* (Wiese et al. 2010; Christensen and Khan 2020a; Mackieh et al. 2021; Ramírez-Castañeda et al. 2026). The extreme resistance observed in some individuals suggests that populations of *E. reginae* may be exposed to high concentrations of one or more of these toxins (Pearson and Tarvin 2022; Ramírez-Castañeda et al. 2026). Because GC–MS cannot detect TTX, its presence is uncertain in *A. trivittata* or other frogs previously surveyed with GC–MS but not LC–MS (Pearson and Tarvin 2022).

In contrast, we found that *Er*$Na_V1.4$-R was sensitive to *A. trivittata* to frog skin secretions and to PTX **251D** and H8-HTX individual dendrobatid alkaloids. Thus, the *Er*$Na_V1.4$-R does not have TSR to these toxins. However, we cannot rule out the possibility that other molecular targets have amino acid substitutions that provide TSR, given that some *A. trivittata*-derived toxins target nicotinic acetylcholine receptors and voltage-gated potassium channels (Daly and Spande 1986; Vandendriessche et al. 2008). A computational assessment suggested that the most common target of poison frog alkaloids may be muscarinic acetylcholine receptors (Yeager et al. 2024).

Liver activity contributes resistance to *A. trivittata* toxins and neoSTX

Once toxin ingestion occurs, predators rely on resistance mechanisms that involve metabolizing the toxin or modifying its target, i.e., TSR (Tarvin et al. 2023). Above, we demonstrate that *E. reginae* has TSR in its $Na_V1.4$ channel to TTX, STX, and neoSTX, but not to the tested frog toxins. We thus endeavored to identify proteins implicated in toxin metabolism by studying the liver, the primary organ responsible for

detoxification. Liver extract from *M. musculus* had no impact on any toxin or skin secretion. In contrast, liver extract from *E. reginae* was able to counteract a portion of the blocking effect for all poison frog alkaloids and both frog skin extractions, with especially high recovery for HTX **283A**. Liver neutralization represents the first known resistance mechanism to any HTX. Both *C. tenuis* and *E. reginae* livers were able to counteract the impacts of neoSTX, suggesting that liver detoxification of neoSTX could be widespread in snakes, or at least in colubrids; studies of additional snake species are necessary to test this pattern. Because *C. tenuis* was unable to counteract any other toxin, we suggest that *E. reginae* detoxification activity is ecologically specific, targeting toxins present in *A. trivittata*. Although this study shows that *E. reginae* liver extracts did not affect block by TTX and STX, our findings demonstrate that *E. reginae* employs TSR resistance strategies to counteract these compounds.

While total protein amount was standardized for these assays, the identity, relative abundance and affinities of the proteins contributing to liver detoxification are currently unknown. Two main types of soluble proteins could help ameliorate toxin block: 1) enzymes that metabolize toxins and 2) toxin-binding proteins that prevent the toxin from accessing its target but do not alter the toxin's structure (Tarvin et al. 2023). As far as we are aware, there is no metabolic enzyme known to break down any of the tested toxins, although several CYP450s and GSTs are differentially expressed in response to toxin ingestion in poison frogs (O'Connell et al. 2021). In contrast, several toxin-binding proteins for these compounds have been identified: saxiphilin (Sxph), which binds STX and is found in many frogs (Mahar et al. 1991; Morabito and Moczydlowski 1995; Yen et al. 2019; Chen et al. 2022); the Pufferfish saxitoxin and tetrodotoxin binding protein (PSTBP) found in pufferfish (Yotsu-Yamashita et al. 2001). Radiolabelled STX binding studies have also suggested the presence of STX-binding proteins in reptiles, amphibians, fish, and arthropods (Llewellyn et al. 1997; Tarvin et al. 2023). Other general binding proteins include serpins (Alvarez-Buylla et al. 2023), transferrin-like proteins (TF, TFRC, TFR2, TFIP11) (Barabas and Faulk 1993; Tortorella and Karagiannis 2014; Ruiz-Mazón et al. 2024), and lactotransferrin-like proteins (LOC139173594) (Tortorella and Karagiannis 2014). None of these genes were upregulated in the livers of snakes that consumed *A. trivittata*. One, however, showed significant upregulation (SERPIN6, adjusted p-value < 0.05) in snakes fed *S. ruber* (Fig. S6C). This pattern does not rule out constitutive expression of toxin-binding proteins.

In addition to the protein activity demonstrated with the liver extract assays, we found that transporters were upregulated in *E. reginae* following poison frog ingestion (Fig. 5C). One of the gene families with the multiple upregulated genes was SLC, which is widely known for absorption, uptake, and clearance of xenobiotics and drugs (Nigam 2015; Pizzagalli et al. 2021). Non-synonymous substitutions in SLC genes have been linked to altered substrate specificity and efficiency (Han et al. 2011; Engström et al. 2013; Yee et al. 2013). Such mutations may underlie evolutionary adaptations that enable predators like *E. reginae* to regularly consume chemically defended prey without succumbing to their most toxic effects. For example, the upregulated gene *SLC22A7* encodes a known organic anion transporter involved in hepatic excretion of toxins and metabolites in humans, including the plant and amphibian pyrrolizine toxins (Enge et al. 2021; Waizenegger et al. 2021). Other upregulated solute carriers included *SLC15A1*, involved in peptidomimetic uptake (Kawai et al. 2020), and transporters such as *SLC1A5, SLC16A6,* and *SLC5A12,* linked to amino acid and monocarboxylate metabolism (Nigam 2015). *ABCA12* and *NPC1L1*, known lipid and cholesterol transporters (56–58), were also upregulated in *E. reginae* after consumption of *A. trivittata*. Given their role in lipophilic molecule transport, these proteins may contribute to the movement of lipophilic toxins such as HTX and PTX. The upregulated RAB11FIP1, a protein involved in the regulation of intracellular transport vesicles, may play a role in facilitating toxin engulfment, intracellular trafficking, and eventual elimination, potentially contributing to the cellular handling of toxic compounds (Damiani et al. 2004).

Beyond direct detoxification, transporters also play essential roles in maintaining systemic homeostasis. Their increased expression in response to *A. trivittata* ingestion may reflect a broader metabolic stress response, involving inter-organ signaling and physiological adaptation (Nigam 2015). Supporting this idea, we observed overexpression of heat shock proteins in the *A. trivittata* treatment, including *HSPA2* and its associated regulator *HSPBAP1* (Feder and Hofmann 1999) (Fig. S6C). The phospholipase *PLA2G7*, a gene found in the venom of various organisms such as snakes, bees, and scorpions, as well as the

sphingosine-1-phosphate plasma transporter *MFSD2B*, were also highly expressed and are known to be involved in inflammatory responses (Feder and Hofmann 1999; Vu et al. 2017; Spolaore et al. 2019; Li et al. 2021; Candels et al. 2022; Le et al. 2022) (Fig. S6C). These proteins are well-established markers of cellular stress and may signal a generalized physiological response to toxic prey ingestion.

Altogether, our RNA-seq data suggest that transporter overexpression in the liver represents yet another resistance mechanism present in *E. reginae*: toxin elimination. While no previously reported toxin-binding proteins were strongly upregulated after *A. trivittata* consumption, the presence of soluble candidates and upregulation of transmembrane transporters indicate that multiple pathways, including toxin binding, membrane trafficking, and metabolic elimination, jointly contribute to toxin resistance in *E. reginae*. Together, these findings suggest that toxin resistance emerges from shared and inducible detoxification pathways, emphasizing the central role of gene regulation and plasticity in predator responses to toxic prey.

Comparison to other systems

Some of the best studied vertebrates in terms of dietary toxin resistance include garter snakes (genus *Thamnophis*), keelback snakes (genus *Rhabdophis*), poison frogs (Dendrobatidae), and woodrats (genus *Neotoma*). Most work on *Thamnophis* species has focused on TSR and whole-organismal measurements of resistance (Brodie et al. 2002; Geffeney et al. 2005; McGlothlin et al. 2014; Hague et al. 2018); one study on *T. elegans* also demonstrated changes in gene expression of sodium-potassium pumps following consumption of toxic toads (Mohammadi et al. 2017). Another study demonstrated convergent enlargement of adrenal glands in *Rhabdophis tigrinus* and other toad-eating snakes (Mohammadi et al. 2013); subsequent work further showed that *R. tigrinus* deploys hormonal regulation and chemical biotransformation of sequestered bufadienolides (Mohammadi et al. 2017; Inoue et al. 2021). Woodrats in the genus *Neotoma* have undergone multiple gene duplications and increased overall expression of several types of digestive enzymes in the glucuronidation pathway that help them deal with toxins from their creosote diet (Klure et al. 2025). Further, woodrats (and many other mammals) have resistance to snake venom through binding proteins (Perez et al. 1978; Biardi et al. 2011) and/or TSR (Voss and Jansa 2012). Among invertebrates, this is perhaps best illustrated by the copepod *Calanus finmarchicus*, which when consuming the STX-producing dinoflagellate express TSR splice variants alongside diet-induced upregulation of digestive enzymes (Roncalli et al. 2017). Monarch butterflies (*Danaus plexippus*) offer a complementary example across multiple compounds within a single toxin class: they resist cardenolides through a combination of Na^+/K^+-ATPase target-site mutations, selective sequestration, metabolic detoxification, and transporter-mediated trafficking, with the specific mechanism varying by cardenolide (Jones and Agrawal 2019; Agrawal et al. 2021). These examples hint at a broader pattern: organisms exposed to dietary toxins frequently evolve more than one physiological strategy to manage them, whether acting on the same toxin through redundant mechanisms or partitioning different mechanisms across chemically distinct compounds. Yet, clear demonstration of multiple mechanisms of resistance to multiple dietary toxins in a single system – as we describe for *E. reginae* – are rare. This is partly because presumably some organisms genuinely interact with only one toxin (e.g., *Thamnophis* snakes (Brodie and Brodie 1990)), but it is also a product of single-toxin research frameworks (van Thiel et al. 2022). Such studies have revealed incredible convergence in the same toxin resistance mechanisms across broad phylogenetic scales, such as convergent amino acid changes in voltage-gated sodium channels that provide resistance to TTX (Toledo et al. 2016) or substitutions in sodium-potassium pumps that provide resistance to cardiotoxic steroids (Ujvari et al. 2015).

Among vertebrates, dendrobatid poison frogs present the most compelling parallel to the multi-toxin scenario: they encounter dozens of alkaloid classes from arthropod prey and appear to deploy a combination of target-site resistance, alkaloid-binding plasma proteins, and active sequestration, sometimes deploying different mechanisms for different compounds within the same individual (Tarvin et al. 2017; Caty et al. 2019; O'Connell et al. 2021; Alvarez-Buylla et al. 2023; Jeckel et al. 2026). Analogous multi-mechanism resistance has been described in vertebrate predators of venomous snakes, where the

inherent chemical complexity of venom, typically a cocktail of metalloproteinases, phospholipases, neurotoxins, and coagulopathic lectins, demands resistance to multiple toxin classes simultaneously. Opossums (*Didelphis* spp.) deploy both toxin-neutralizing serum glycoproteins targeting metalloproteinases and phospholipase A_2, and adaptive TSR-like mutations, distinct mechanisms acting on different components of the same venom (Jansa and Voss 2011; Voss and Jansa 2012). Mongooses (*Herpestes* spp.) similarly combine nAChR target-site mutations against α-neurotoxins with serum metalloproteinase inhibitors (Drabeck et al. 2015).

The present study is among the first to investigate the physiological implications of exposure to multiple dietary toxins and to characterize the diverse adaptive mechanisms a predator deploys to manage them. *Erythrolamprus reginae* is not the first snake to consume toxic prey without being a dietary specialist on it (e.g. (Mohammadi et al. 2016)), nor the first to harbor target-site resistance mutations (McGlothlin et al. 2016; van Thiel et al. 2022), nor the first organism to express detoxifying enzymes or toxin-binding proteins (e.g. (Chen et al. 2022)). What we demonstrate here, however, is that a single organism employs these distinct mechanisms, sometimes in concert, to contend with a diverse toxin landscape. NeoSTX, for example, appears to be counteracted by two independent resistance mechanisms: liver-expressed proteins that neutralize the toxin through an unknown process (Fig. 2F) and TSR-associated mutations in $Na_V1.4$. On the other hand, TTX and STX resistance appears to be mediated primarily through TSRs, while HTX and PTX resistance involves liver protein-mediated neutralization, although TSR involvement for these toxins has not been excluded. Additionally, exposure to toxic prey elicits elevated transporter expression, implicating both constitutive genetic and inducible transcriptional components in a multimodal resistance system. Despite the presence of toxin resistance mechanisms to deal with guanidinium toxins, the ecological sources of TTX, STX, and neoSTX exposure remain unknown for *E. reginae*. TTX and STX occur broadly in amphibians and freshwater cyanobacteria, respectively, but neither source has yet been confirmed in the Amazon (Hanifin 2010; Christensen and Khan 2020b; Mackieh et al. 2021; Deng et al. 2025). Thus this study reveals that the diversity of toxin-producing organisms and predator–prey chemical interactions in Amazonian forests is likely underestimated. The complex trophic networks characteristic of tropical rainforests extend to an equally complex chemical landscape involving toxin producers, toxin predators, and toxin sequestration, all of which represent important selective forces. As forest complexity declines, the erosion of these chemical interactions may function both as an indicator and as an accelerating factor in the loss of organismal biodiversity.

Conclusion

Our findings characterize the coexistence of multiple toxin resistance mechanisms in *E. reginae* from Leticia, Colombia. In contrast to prior reports, we documented behavioral avoidance towards toxic prey, as well as a novel dragging behavior in *E. reginae*. In addition, this population exhibits both TSR in $Na_V1.4$ and liver-mediated detoxification, highlighting the integrative nature of toxin resistance and its ability to counteract complex chemical defenses. This coexistence highlights both the intense physiological demands of feeding on multiple toxic prey and the adaptive advantage of integrating complementary resistance strategies. In summary, our study highlights toxin resistance as a multiscale phenotype shaped by the interaction of behavior, physiology, and molecular evolution, revealing how complementary resistance strategies enable predators to persist in chemically complex ecosystems.

Materials and Methods

Animal collection

We collected 12 *Erythrolamprus reginae* snakes, 6 *Ameerega trivittata* frogs, and 6 *Scinax ruber* frogs from Leticia, Amazonas, Colombia (Table S1). These specimens were captured by hand or using a snake hook. Collection permit was granted by the Colombian Authority for Environmental Licenses (ANLA; No. 1249, 23 July 2020, RCI0002-00-2020). To avoid any impact of chemical euthanasia on our results, we euthanized snakes by decapitation followed by rapid extraction of the brain tissue. Frogs were euthanized using hypothermic shock. Euthanasia and predation trial (below) protocols were approved by the IACUC

No. AUP-2019-08-12457-1 issued by the University of California, Berkeley. Non-CITES tissue samples were exported under the ANLA permits No. 02191, No. 02376, and No. 3271. For *A. trivittata* the exportation of the tissues was granted by the CITES export permits No. CO26165 and No. CO46959.

Predation Behavior Test

We hand or snake-hook captured snakes and housed them individually close to the site of capture in mesh cages (30 cm x 30 cm from RestCloud) with water, and natural leaves, ground, and hiding spots (log cylinders) for an acclimatization period of five days. This period ensured that the digestive tracts of the snakes were empty before the experiment. The anurans were collected one or two days before each trial and kept under the same mesh cages conditions. We video-recorded using a Nikon D5600 camera *E. reginae* predation events against the poisonous frog *A. trivittata* (Dendrobatidae) and the non-poisonous *S. ruber* (Hylidae; Dataset S1 & Dataset S2). If after 2 hours the toxic frog was not ingested, we removed the toxic frog, and a second frog—*Leptodactylus* sp., *Sphaenorynchus lacteus, Dendropsophus* sp., *Rhinella margaritifera*, or *Scinax ruber*—was introduced to the enclosure to determine whether the snake was generally unwilling to eat or specifically rejected *A. trivittata* (see Fig. 1A). All offered frogs are natural prey of *E. reginae*, ensuring that the experiment simulated natural feeding conditions.

During the experiment, the snake and posteriorly the frog were introduced into an empty mesh enclosure. We recorded the interaction until 40 minutes after ingestion or vomiting of the frog, or up to two hours if no ingestion occurred. If no predation was observed, the trial was terminated after two hours. Predation events were classified as "ingested," "vomited," or "avoided" following Brodie and Tumbarello (Brodie and Tumbarello 1978). Snakes were euthanized 40 minutes after the frog was completely swallowed to obtain tissue samples for transcriptome analysis. According to Williams et al. (Williams et al. 2010), toxin intoxication effects become measurable within 30–40 minutes post-ingestion. Video recordings were analyzed to document notable behaviors, including the time elapsed from the first attack to the moment the frog was fully swallowed ("Time to swallow") and the number of times the snake exhibited dragging behavior ("Dragging cycles"). We define dragging behavior as the act of swabbing or rubbing the frog, already held in the snake's mouth, along the floor or wall. Each dragging cycle was counted from the moment the snake began dragging to when it paused, rather than based on the number of physical drags performed.

Transcriptome

RNA library preparation

Snakes were sacrificed after each predation experiment (*A. trivittata* or *S. ruber* ingestion) or after a 5-day fasting period (control; Table S2). Snake tissues were collected in the field, stored in RNA later, and transported for a longer storage at -80 °C freezer (Table S2). For RNA extraction, we used the Monarch® Total RNA Miniprep Kit from NEB Biolab and followed the protocol for <10 mg initial tissue. The homogenization of the tissues was performed using the PowerLyzer™ 24 bead beater (MO BIO Laboratories, Inc.), with two cycles of 3500 RPM for 45 seconds, each followed by a 30-second rest period, and an intermediate speed of 3500 RPM. To assess starting RNA quantity and quality, we used the Qubit RNA HS Assay Kit from ThemoFisher Scientific and Bioanalyzer RNA Analysis from Agilent.

For the RNA library prep, we selected the high quality RNA samples (RIN ≥ 7) with up to 500 ng RNA, except for a few irreplaceable samples that had low RIN scores despite several extraction attempts. We followed a poly(A) selection protocol for all samples using the Watchmaker mRNA Capture Kit from Watchmaker Genomics. For the library amplification, seven extra cycles were used for the low RIN score samples (Table S2). RNA libraries were sequenced to obtain ~30 M paired-end reads (150 bp) per tissue on a Illumina NovaSeq™ X 10B flow cell. Raw data is available in (Bioproject PRJNA1274516, see complete biosample numbers in table S1).

RNA-seq data processing and analysis

Raw paired-end RNA-seq reads were quality-filtered and trimmed using fastp v0.23.2 (Chen 2023) with adapter detection enabled and default settings. Cleaned reads were aligned to the *E.reginae* reference genome (GCF_031021105.1) using HISAT2 v2.2.1 (Kim et al. 2015) with the *--dta* flag to facilitate

transcript assembly. Alignment outputs in SAM format were converted to BAM, sorted, and indexed using Picard and samtools v1.21 . Alignment quality metrics were generated with the *flagstat* tool. The genome annotation file (GFF) was converted to GTF format using gffread (Pertea and Pertea 2020), with manual correction of gene identifiers to ensure compatibility with downstream quantification tools. Transcript abundance was quantified using HTSeq-count v0.13.5 (Putri et al. 2022) in unstranded mode (-s no) with exon-level features and gene-level aggregation (-i gene_id).

Transcript abundance data were analyzed using DESeq2 in R (v4.3.0) (Love et al. 2014). Count matrices from HTSeq-count were merged and filtered to include genes expressed in digestive tissues: liver, tongue, stomach, and intestine. These tissues were obtained from 3 different feeding treatments (see above): after 5 days fasting, or 40 minutes after the ingestion of an *A. trivittata* or *S. ruber* prey. Differential gene expression (DE) analyses were performed using DESeq2 with tissue and condition as covariates (see dataset S3: log2fold and p-value results). Principal component analysis (PCA) and volcano plots were generated to assess sample clustering and DE genes (Fig. S7). Genes with adjusted p-value < 0.05 and log2FoldChange > 0 were considered significant and upregulated (Dataset S3). The final list of upregulated genes for each condition was compiled by combining DE genes identified across the three pairwise comparisons: fasting vs. *A trivittata*, fasting vs. *S. ruber*, and *S. ruber* vs. *A. trivittata*. For the expressed gene counts, we retained only protein-coding genes from the set of upregulated transcripts by filtering the set of upregulated genes by *E. reginae* gene identifiers from the NCBI genome annotation classified as protein-coding. To investigate functional patterns of gene expression across conditions, we classified differentially expressed genes into biologically relevant categories based on gene name patterns and annotations. Using regular expressions, we extracted gene sets associated with specific protein families and functional categories from the differential expression results.

Gene categories related to toxin resistance were used to highlight potential differential expression of these genes in the volcano plots (Fig. S7). We grouped solute carrier family genes (SLC), phospholipase A2 genes (PLA2), cytochrome P450 genes (CYP), serine protease inhibitors (SERPIN), ATP-binding cassette transporters (ABC), heat shock proteins (HSP), and Rab GTPases (RAB) based on their gene name prefixes. Transferrin-related genes (TF, TFRC, TFIP11, and TFR2) were grouped using known gene symbols. Cholinesterase-like genes (*E. reginae* transcript IDs: LOC139158370–LOC139158371, LOC139159376, LOC139160160, LOC139160166, LOC139160209–LOC139160211, LOC139160214–LOC139160215, LOC139160217, LOC139160219–LOC139160220, LOC139160232), lactotransferrin-like gene (ID: LOC139173594 and LTF) and 85 transporters genes (Data S8) were manually identified using the ncbi gene annotations of *Erythrolamprus reginae* (GCF_031021105.1).

Functional enrichment of DE genes was assessed using topGO (ontology: Molecular Function) (Alexa and Rahnenfuhrer 2022). Gene-to-GO mappings were obtained using *Anolis carolinensis* annotations (Unitprot taxon ID 28377). Only genes with detectable expression across samples (mean normalized counts > 0.5) were used as background. Enrichment results were visualized using the molecular function option “MF” and cellular component option “CC”.

Skin secretion GC-MS toxin profile analysis

Following euthanasia, we removed entire skins from 6 *A. trivittata* and 6 *S. ruber* and placed each in ~1 mL 100% ethanol in glass vials with PTFE-lined caps and stored at -80 °C. A 100 µL aliquot of the solution was sampled and analyzed directly by Gas-Chromatography Mass-Spectrometry (GC-MS). Samples (1 µL) were analyzed using either a Thermo iTQ1100 unit resolution ion trap instrument or Thermo Exploris GC high-resolution orbitrap instrument. GC separation used 5% phenyl methylsilicone columns (Restek RTX-5MS or Thermo TG-5Si, 0.25 mm x 30m, 0.25 µm film thickness) with splitless injection with a ramp from 100C to 280C as previously described (Tarvin et al. 2024). Retention indices (Kovats) were determined by comparison to alkane standards injected with the group. Samples were sequentially analyzed in electron ionization (EI) and chemical ionization with ammonia reagent gas (CI-NH_3). Compounds were identified by comparison with EI library spectra, molecular weight/formula match, and retention index.

Toxin sources and preparation for electrophysiology analyses

STX was synthesized as described (Andresen and Bois 2009). Neosaxitoxin (neoSTX) was purchased from Sigma Aldrich (Sigma-Aldrich GmbH, Switzerland, cat. no. 41619). Tetrodotoxin citrate (TTX) was purchased from Cayman Chemical (MI, USA, cat. no. NC1735928). All toxins were lyophilized and dissolved in ultrapure water in stocks of 1–5 mM for further use.

From the original 100% ethanol solution containing whole-skin extracts of *A. trivittata* and *S. ruber*, 100 µl was taken from each individual skin sample to create a combined 600 µl skin secretion solution for each species. Ethanol was evaporated using a low-pressure nitrogen flow in a Rotavapor R-300 vacuum system (100 mbar, 35 °C). The resulting solute was then resuspended in 30 µl of ultrapure water containing 5% DMSO to facilitate the dilution of hydrophobic compounds. A 1:1000 dilution was used in the TEVC assays, determined by the low final volume available to conduct repetitions.

Another five toxins found in dendrobatid frogs were shared by the Fitchlab (coauthor) from the John W. Daly laboratory collection (John W. Daly 1995). Decahydroquinoline **195A** (DHQ **195A,** aka PTX-C, PTX-C_I), Synthetic racemic DHQ **167** HCl, (aka PTX-C_{IV}) was a generous gift of Dr. Larry Overman (Overman and Jessup 1978). Synthetic (+)-PTX **251D** HCl was prepared as described (Daly et al. 2003). Racemic octahydrohistrionicotoxin HCl (H_8-HTX, HTX **291A**) was a generous gift of Dr. Yoshito Kishi (94). Natural histrionicotoxin (HTX **283A**) was isolated from mixed frog collections (Daly et al. 1971). These toxins were diluted in ultrapure water or ultrapure water plus 5% DMSO to obtain a 30nM to 100 nM stock dilution (Table S3).

Generating liver soluble protein extracts

E. reginae (n = 2) and *C. tenuis* (n = 1) specimens were collected and euthanized according to approved UCB IACUC protocols (AUP-2019-08-12457) and a California Department of Fish and Wildlife Collecting Permit S-190980001-19111-001 (Table S1). Animals were humanely euthanized via decapitation, and liver samples were immediately dissected, flash-frozen, and stored at -80°C. Control mouse liver samples were collected from 5–6-week-old female CD1-IGS mice (Charles River Laboratories, Wilmington, MA, USA) under UCSF IACUC protocol AN076215-01F, and immediately flash-frozen in liquid nitrogen and stored at -80°C. Liver homogenization was adapted from descriptions of isolating soluble toxin-binding proteins from animal tissues by Llewellyn et al. (Llewellyn et al. 1997; Llewellyn et al. 1998). In brief, livers were homogenized at approximately 1 ml per g of tissue in a buffer consisting of 10 mM Tris-HCl, 0.2 mM ethylenediaminetetraacetic acid (EDTA), pH 7.4, supplemented with EDTA-free protease inhibitor tablets (ThermoFisher Scientific, Waltham, MA, USA, Cat. A32955). Livers were homogenized using a PowerLyizer™ 24 bead beater with two cycles of 3500 rpm for 45 seconds, 30 seconds rest, and 3500 rpm for 45 seconds. Liver extracts were then centrifuged at 10,000 *g* for 15 minutes and the resultant pellet was discarded. The supernatant was filtered and then flash-frozen and stored at -80°C until use. Total protein was measured using the Pierce binchoninic acid (BCA) protein assay (ThermoFisher Scientific, cat. no. 23225) and extracts standardized to 0.2 mg/mL final concentration.

Mammalian cell culture

Chinese hamster ovary (CHO) cells stably expressing the α-subunit of the human skeletal muscle sodium channel isoform (*Hs*$Na_V1.4$, NM_00334.4, B'SYS GmbH, cat. no. BSYS-NaV1.4-CHO-C) were maintained at 37°C, 5% CO_2 in culture medium containing Ham's F-12 medium with GlutaMAX (Gibco, cat. no. 31765035) supplemented with 9% (v/v) heat-inactivated fetal bovine serum (Gibco, cat. no. 16140071), penicillin-streptomycin (0.9% (v/v), Gibco, cat. no. 15-140-122) and 100 µg/mL Hygromycin B (Sigma-Aldrich, cat. no. 10843555001).

Whole-cell patch-clamp electrophysiology

The effects of treating toxins with liver extract on *Hs*$Na_V1.4$ were assessed using a semi-automated QPatch Compact II electrophysiology platform (Sophion Bioscience, Ballerup, Denmark). Recordings were conducted at 22°C. The intracellular solution (IC) contained the following in mM: 140 CsF, 1/5 EGTA/CsOH, 10 HEPES, 10 NaCl (pH 7.3 with 3M CsOH), 320 mOsm. The extracellular solution (EC, saline) contained the following in mM: 2 $CaCl_2$, 1 $MgCl_2$, 4 KCl, 145 NaCl, 10 HEPES, 10 glucose (pH 7.4 with NaOH), 305 mOsm. Solutions were filtered using a 0.22 µM membrane filter.

Before recording, cells were washed with Dulbecco's phosphate buffered saline (DPBS, Gibco, cat. no. 14190144), detached from culture flasks with Detachin (AMSBIO, cat. no. T100100) and then kept in serum-free medium (Sigma-Aldrich, cat. no. C5467) supplemented with 25 mM HEPES and 0.04 mg/mL soybean trypsin inhibitor (Sigma-Aldrich, cat. no. 10109886001). Immediately prior to recording, cells were washed and resuspended in EC to a final cell density of 4–6 x 10 cells/mL, and then applied to the QPatch Compact II (Sophion Bioscience, Ballerup, Denmark) using 8-channel QPlate 8X multihole chips (Sophion Bioscience, cat. no. SB0210).

Sodium currents were acquired at 25 kHz and filtered at 8333 kHz, with leak subtraction protocol applied and non-leak subtracted currents acquired in parallel. Sodium currents were elicited using a single pulse protocol where cells were held at -90 mV, with a hyperpolarization step of -120 mV for 200 ms followed by a depolarization step to 0 mV for 60 ms and then returned to a holding potential of -90 mV, with sweep-to-sweep interval duration of 10 seconds. All recordings were conducted at 22°C.

The effect of guanidinium toxins alone on *Hs*Na_V1.4 in CHO cells were first assessed by determining cumulative toxin concentration-response curves, with toxin solutions prepared in 3-fold serial dilution series in EC and applied as increasing concentrations. The IC_{50} concentrations were calculated by fitting the concentration-response curves with non-linear regression models in GraphPad Prism V10.0. Toxin concentrations sufficient to block ~90% of *Hs*Na_V1.4 currents were subsequently calculated using the IC_{50} and hillslope (*H*) as follows: ICx =(x100-x)1HIC50. The half-maximal inhibitory (IC_{50}) values for the human skeletal muscle Na_V channel (*Hs*Na_V1.4) were in line with previous studies (Fig. S2) (Alonso et al. 2016; Zakrzewska et al. 2025).

The effect of incubating toxin in liver extract was assessed by diluting samples in EC containing 0.05% *w/v* bovine serum albumin (BSA) and then incubating at room temperature (23 ± 2°C) for 30 min. Samples included: toxin alone; toxin combined with liver extract (0.2 mg/mL final); and liver extract alone (0.2 mg/mL). Where possible, toxin concentrations were selected with the aim of inhibiting 90% of sodium currents, which were calculated from the toxin concentration-response curves to be approximately 1.5 nM for neoSTX, 100 nM for STX, and 300 nM for TTX. In the case of frog-derived alkaloids, where toxin quantities were exceedingly limited, a single high concentration able to block putatively resistant *Erythrolamprus reginae Er*Na_V1.4 by at least 60% was selected: 250 µM H_8-HTX; 500 µM HTX283A; 500 µM PTX251D; and *A. trivittatta* skin extract (1:200 dilution). After incubating, these samples were applied to *Hs*Na_V1.4 cells, in stable whole-cell patch-clamp configuration with minimum of 1 nA of sodium current, in a successive fashion. First, steady baseline sodium currents were established in EC, followed by inhibiting currents with toxin-alone. Toxin samples were then washed out until currents returned to baseline, using at least nine chamber volumes of EC. The toxin:liver extract mix was then applied and compared against currents elicited in EC and toxin alone solutions. Finally, the toxin:liver extract mix was washed out and then liver extract alone was applied as a control. See Fig. S3 for schematic of assay. All liver extracts and toxins were screened at minimum in duplicate in two independent assays. Normalized current recovery was then determined using the following equation: , where $I_{control}$ is the baseline current elicited in EC, I_{toxin} is the current after application of toxin alone, and $I_{toxin:liver}$ is the current following application of the mixed toxin:liver extract. The degree of current recovery for each toxin between different species of liver extract was compared by one-way ANOVA with Tukey's post hoc test. All data analyses were performed using Sophion Analyzer software (Sophion Bioscience) and GraphPad Prism v10.0 (GraphPad Prism, San Diego, CA, USA).

Gene Reconstruction and Cloning of E. reginae Na_V1.4 (NR & R) and HsNa_V1.4

We used the *E. reginae* complete Na_V1.4 gene reconstruction from sample No. GECOH 2823 collected in Santa María, Boyacá, Colombia, with complete information published in (Ramírez-Castañeda et al. 2026), as the template. Minor gaps in the sequence were completed using transcriptome samples generated in this study, employing BLAST v2.7.1+ to identify the required sites (Altschul et al. 1990).

Gene synthesis and cloning into the pcDNA3.1+ vector were requested from GenScript USA Inc. for two sequences: a non-resistant variant and a resistant variant of the *E. reginae* Na_V1.4 channel, following the

sequences published in (Ramírez-Castañeda et al. 2026) (*Er*Na_V1.4-NR and *Er*Na_V14.-R) (see Fig. S1 & complete sequences in Dataset S4). Additionally, we ordered the complete synthesis and cloning of the human Na_V1.4 channel into pcDNA3.1 from the same company (Ref=CCDS:CCDS45761.1, protein_id=NP_000325.4) (*Hs*Na_V1.4; GenScript USA Inc.) (complete sequences in Dataset S4). Nomenclature to highlight amino-acid homologous positions is based on the human Na_V1.4 sequence.
In initial trials, the ErNa_V1.4 (NR) and ErNa_V1.4 (R) constructs were found to be unstable during replication. To address this, we used CopyCutter™ EPI400 Chemically Competent *E. coli* cells from VWR International and followed the recommended protocol.

Two-electrode voltage-clamp electrophysiology (TEVC)
Two-electrode voltage-clamp (TEVC) recordings were conducted using defolliculated *Xenopus laevis* oocytes at developmental stages V–VI. Oocytes were harvested following the AN178461 IACUC protocol, with recordings performed 1–2 days after microinjection with *Hs*Na_V1.4 mRNA and 3–4 days post-injection for *E. reginae* Na_V1.4 (NR & R). Linearized cDNA constructs were transcribed into capped mRNA using the mMESSAGE mMACHINE T7 Transcription Kit (Invitrogen). Microinjections were performed using 9–16 ng of *Hs*Na_V1.4 mRNA and 50–64 ng of *E. reginae* Na_V1.4 (NR & R) mRNA. Data acquisition was carried out using a GeneClamp 500B amplifier (MDS Analytical Technologies) controlled by pClamp software (Molecular Devices), with signals digitized at 1 kHz using a Digidata 1332A digitizer (MDS Analytical Technologies). Oocytes were impaled with borosilicate glass microelectrodes (0.3–3.0 MΩ resistance) filled with 3 M KCl. Sodium currents were recorded in a bath solution (RS) composed of 96 mM NaCl, 1 mM CaCl2, 1 mM MgCl2, 2 mM KCl, and 5 mM HEPES (pH 7.5, adjusted with NaOH).
To determine the concentration–response relationship for STX, TTX, and neoSTX, test solutions containing specific toxin concentrations were sequentially applied via perfusion to oocytes expressing the channels (n = 6 oocytes, per Na_V channel and toxin). Sodium currents were elicited using a single-pulse protocol where oocytes were held at -120 mV for 3 s, followed by a depolarization step to 0 mV for 60 ms, before returning to -120 mV. The interval between sweeps was 10 s.

For STX and TTX, toxin block was washed out between concentrations (approximately 20 sweeps). For neoSTX, a cumulative toxin recording approach was used, where each concentration was maintained for ~50 sweeps. The IC_{50} values (Fig. 2 and Table S4), representing the toxin concentration required to inhibit 50% of the current, were calculated by fitting concentration-response curves based on the ratio of peak currents in the presence and absence of toxin using the equation:
Ix=(Imax−Imin)I0(1+ICxIC50)I_x = \frac{(I_{max} - I_{min})}{I_0 (1 + \frac{IC_x}{IC_{50}})} where *Ix* represents the current amplitude at toxin concentration *x*, *I0* is the current amplitude in the absence of toxin, and *I_{max}* and *I_{min}* correspond to the maximum and minimum peak current amplitudes, respectively.

Due to the limited availability of skin secretions and other dendrobatid toxins, a single toxin concentration was applied to the TEVC chamber for single-pulse recordings, followed by washout with buffer for ~50 sweeps (n = 3 oocytes per Na_V channel and toxin). The following toxin concentrations were used: a 1:100 dilution of *A. trivittata* and *S. ruber* skin extract, 500 µM H8-HTX, 500 µM HTX, 500 µM PTX251D, 1000 µM DHQ195A, and 1000 µM DHQ167. The available toxin quantities were insufficient to conduct tests with multiple concentrations. For statistical analysis, a non-parametric Mann-Whitney test was used to compare the reduction in current in the presence and absence of the toxin.

Activation and inactivation properties of each expressed Na_V channel were determined using specific voltage protocols. Inactivation was measured by holding the membrane potential at -120 mV for 30 ms, followed by incremental 10 mV depolarization steps for 600 ms, ending with a final step to 0 mV for 30 ms before returning to -120 mV. Activation was assessed by first applying a hyperpolarization step to -100 mV for 6.5 ms, followed by a depolarization from -100 mV to 70 mV by incremental 5 mV depolarization steps for 60 ms before returning to -120 mV.

Acknowledgments

We thank the Russell E. Train Education for Nature Program (EF14103) from the World Wildlife Fund (WWF), the National Institutes of Health (NIGMS #R35GM150574 to RDT, NIGMS 1S10GM154292-01 to RWF), National Science Foundation (DUE-0942345, IOS-1556982 to RWF), the MVZ Wake Research Award, and the GRAC Research Funds from the Integrative Biology Department at UC Berkeley, which supported VRC's expenses during field collection, analysis, and writing. This work was partially supported by grants DoD HDTRA-1-19-0040, HDTRA-1-21-1-0011, and HDTRA-1-23-0026 to DLM. Thanks to José Rances Caicedo Portilla and Martha Calderón for all your help during the animal collection process. We are very grateful to all the members of the Minor Lab and the Tarvin Lab for their help during the electrophysiology experiments, and to the EGL Laboratory and QB3 Genomics, especially Lydia Smith, for your dedicated support during the transcriptome library preparation. We thank J. Du Bois for supplying STX samples. Special thanks to José Guillermo Díaz Cahuachi, Ana Milena Castro, Francy Silva, the Kuiru family (Mirna Kuiru, Luna, Marco, and Camila), and the Naforo-Bautista family (Maritza Naforo Bautista, María Bautista Pinto, Juan Naforo Bautista, Orfilia Gomez, Velentina) for your knowledge, kindness, and invaluable help during sample collection, predation experiments, and in general, for making this research possible. We thank Reserva Maiku in Puerto Nariño and the Hermanos Menores Capuchinos de Leticia for granting us permission to work on their lands. We are deeply grateful to all the local guides and workers who assisted us and generously shared their time and knowledge. We are also thankful for the opportunity to observe and interact with snakes and frogs, to witness them up close, and to share a home with them, the forest, and the cities where they live. We acknowledge that our fieldwork was conducted in territories where local communities have historically faced limited participation in science and continue to experience the effects of extractive practices. We are committed to conducting this work with equity and respect, and hope its findings will contribute to the well-being of the communities and environments involved. The Spanish translation was produced using Claude and edited by VRC (Available in Dataset S7) (Anthropic 2026).

Data and materials availability: Transcriptome raw data is available in Bioproject PRJNA1274516, see complete biosample numbers in table S1. Transcriptome code is available in https://github.com/esperando370/Ereginae_transcriptome. GC-MS data is available in MassIVE dataset (MSV000098843). Other data is available in the main text or the supplementary materials.

References

Abderemane-Ali F, Rossen ND, Kobiela ME, Craig RA, Garrison CE, Chen Z, Colleran CM, O'Connell LA, Bois JD, Dumbacher JP, et al. 2021. Evidence that toxin resistance in poison birds and frogs is not rooted in sodium channel mutations and may rely on "toxin sponge" proteins. *J. Gen. Physiol.* [Internet] 153. Available from: https://doi.org/10.1085/jgp.202112872

Agrawal AA, Böröczky K, Haribal M, Hastings AP, White RA, Jiang R-W, Duplais C. 2021. Cardenolides, toxicity, and the costs of sequestration in the coevolutionary interaction between monarchs and milkweeds. *Proc. Natl. Acad. Sci.* [Internet] 118:e2024463118. Available from: https://www.pnas.org/doi/abs/10.1073/pnas.2024463118

Albarelli LPP, Santos-Costa MC. 2010. Feeding ecology of Liophis reginae semilineatus (Serpentes: Colubridae: Xenodontinae) in eastern Amazon, Brazil. *Zool. Curitiba* [Internet] 27:87–91. Available from: http://www.scielo.br/j/zool/a/JzrKsdmm53NMWPDFf4wJz7L/?lang=en

Alexa A, Rahnenfuhrer J. 2022. topGO: Enrichment Analysis for Gene Ontology.

Alonso E, Alfonso A, Vieytes MR, Botana LM. 2016. Evaluation of toxicity equivalent factors of paralytic shellfish poisoning toxins in seven human sodium channels types by an automated high throughput electrophysiology system. *Arch. Toxicol.* 90:479–488.

Altschul SF, Gish W, Miller W, Myers EW, Lipman DJ. 1990. Basic local alignment search tool. *J. Mol. Biol.* 215:403–410.

Alvarez-Buylla A, Fischer M-T, Moya Garzon MD, Rangel AE, Tapia EE, Tanzo JT, Soh HT, Coloma LA, Long JZ, O'Connell LA. 2023. Binding and sequestration of poison frog alkaloids by a plasma globulin.Radhakrishnan A, Schuman MC, editors. *eLife* [Internet] 12:e85096. Available from: https://doi.org/10.7554/eLife.85096

Alvarez-Buylla A, Payne CY, Vidoudez C, Trauger SA, O'Connell LA. 2022. Molecular physiology of pumiliotoxin sequestration in a poison frog. *PLOS ONE* [Internet] 17:e0264540. Available from: https://journals.plos.org/plosone/article?id=10.1371/journal.pone.0264540

Andresen BM, Bois JD. 2009. De novo Synthesis of Modified Saxitoxins for Sodium Ion Channel Study. *J. Am. Chem. Soc.* [Internet] 131:12524–12525. Available from: https://www.ncbi.nlm.nih.gov/pmc/articles/PMC2770901/

Anon. 1986. Alkaloids: Chemical and Biological Perspectives. In: Alkaloids: Chemical and Biological Perspectives. New York: Wiley. p. 1–274.

Anthropic. 2026. Claude 3.7 Sonnet. Available from: https://claude.ai

Aubier TG, Sherratt TN. 2020. State-Dependent Decision-Making by Predators and Its Consequences for Mimicry. *Am. Nat.* [Internet] 196:E127–E144. Available from: https://www.journals.uchicago.edu/doi/10.1086/710568

Barabas K, Faulk WP. 1993. Transferrin receptors associate with drug resistance in cancer cells. *Biochem. Biophys. Res. Commun.* 197:702–708.

Biardi JE, Ho CYL, Marcinczyk J, Nambiar KP. 2011. Isolation and identification of a snake venom metalloproteinase inhibitor from California ground squirrel (*Spermophilus beecheyi*) blood sera. *Toxicon* [Internet] 58:486–493. Available from: https://www.sciencedirect.com/science/article/pii/S0041010111002571

Bricelj VM, Connell L, Konoki K, Macquarrie SP, Scheuer T, Catterall WA, Trainer VL. 2005. Sodium channel mutation leading to saxitoxin resistance in clams increases risk of PSP. *Nature* 434:763–767.

Brodie ED, Brodie ED. 1990. Tetrodotoxin resistance in garter snakes: an evolutionary response of predators to dangerous prey. *Evolution* [Internet] 44:651–659. Available from: http://doi.wiley.com/10.1111/j.1558-5646.1990.tb05945.x

Brodie ED, Tumbarello MS. 1978. The Antipredator Functions of Dendrobates auratus (Amphibia, Anura, Dendrobatidae) Skin Secretion in Regard to a Snake Predator (Thamnophis). *J. Herpetol.* 12:264.

Brodie Edmund D., Ridenhour BJ, Brodie E. D. 2002. The evolutionary response of predators to dangerous prey: Hotspots and coldspots in the geographic mosaic of coevolution between garter snakes and newts. *Evolution* [Internet] 56:2067–2082. Available from: http://doi.wiley.com/10.1111/j.0014-3820.2002.tb00132.x

Candels LS, Becker S, Trautwein C. 2022. PLA2G7: a new player in shaping energy metabolism and lifespan. *Signal Transduct. Target. Ther.* [Internet] 7:1–2. Available from: https://www.nature.com/articles/s41392-022-01052-5

Carle T, Rowe C. 2014. Avian predators change their foraging strategy on defended prey when undefended prey are hard to find. *Anim. Behav.* 93:97–103.

del Carlo RE del, Reimche JS, Moniz HA, Hague MTJ, Agarwal SR, Iii EDB, Jr EDB, Leblanc N, Feldman CR. 2024. Coevolution with toxic prey produces functional trade-offs in sodium channels of predatory snakes. *eLife* [Internet] 13. Available from: https://elifesciences.org/reviewed-preprints/94633

Caty SN, Alvarez-Buylla A, Byrd GD, Vidoudez C, Roland AB, Tapia EE, Budnik B, Trauger SA, Coloma LA, O'Connell LA. 2019. Molecular physiology of chemical defenses in a poison frog. *J. Exp. Biol.* [Internet] 222:jeb204149. Available from: https://doi.org/10.1242/jeb.204149

Cei JM, Erspamer V, Roseghini M. 1967. Taxonomic and Evolutionary Significance of Biogenic Amines and Polypeptides Occurring in Amphibian Skin. I. Neotropical Leptodactylid Frogs. *Syst. Biol.* [Internet] 16:328–342. Available from: https://doi.org/10.2307/2412152

Chen S. 2023. Ultrafast one-pass FASTQ data preprocessing, quality control, and deduplication using fastp. *iMeta* [Internet] 2:e107. Available from: https://onlinelibrary.wiley.com/doi/abs/10.1002/imt2.107

Chen Z, Zakrzewska S, Hajare HS, Alvarez-Buylla A, Abderemane-Ali F, Bogan M, Ramirez D, O'Connell LA, Du Bois J, Minor DL. 2022. Definition of a saxitoxin (STX) binding code enables discovery and characterization of the anuran saxiphilin family. *Proc. Natl. Acad. Sci.* [Internet] 119:e2210114119. Available from: https://www.pnas.org/doi/10.1073/pnas.2210114119

Christensen VG, Khan E. 2020a. Freshwater neurotoxins and concerns for human, animal, and ecosystem health: A review of anatoxin-a and saxitoxin. *Sci. Total Environ.* [Internet] 736:139515. Available from: https://www.sciencedirect.com/science/article/pii/S0048969720330321

Christensen VG, Khan E. 2020b. Freshwater neurotoxins and concerns for human, animal, and ecosystem health: A review of anatoxin-a and saxitoxin. *Sci. Total Environ.* [Internet] 736:139515. Available from: https://www.sciencedirect.com/science/article/pii/S0048969720330321

Daly J. W. 1995. The chemistry of poisons in amphibian skin. *Proc. Natl. Acad. Sci. U. S. A.* [Internet] 92:9–13. Available from: http://www.ncbi.nlm.nih.gov/pubmed/7816854 http://www.pubmedcentral.nih.gov/articlerender.fcgi?artid=PMC42808

Daly John W. 1995. The chemistry of poisons in amphibian skin. 92:9–13. Available from: http://www.pnas.org/content/pnas/92/1/9.full.pdf

Daly JW. 1998. Thirty Years of Discovering Arthropod Alkaloids in Amphibian Skin †. 3864:162–172.

Daly JW. 2005. Nicotinic Agonists, Antagonists, and Modulators From Natural Sources. *Cell. Mol. Neurobiol.* [Internet] 25:513–552. Available from: http://link.springer.com/10.1007/s10571-005-3968-4

Daly JW, Garraffo HM, Spande TF, Clark VC, Ma J, Ziffer H, Cover JF. 2003. Evidence for an enantioselective pumiliotoxin 7-hydroxylase in dendrobatid poison frogs of the genus Dendrobates. *Proc. Natl. Acad. Sci.* [Internet] 100:11092–11097. Available from: https://www.pnas.org/doi/10.1073/pnas.1834430100

Daly JW, Karle I, Myers CW, Tokuyama T, Waters JA, Witkop B. 1971. Histrionicotoxins: Roentgen-Ray Analysis of the Novel Allenic and Acetylenic Spiroalkaloids Isolated from a Colombian Frog, Dendrobates histrionicus. *Proc. Natl. Acad. Sci.* [Internet] 68:1870–1875. Available from: https://www.pnas.org/doi/10.1073/pnas.68.8.1870

Daly JW, Myers CW, Whittaker N. 1987. Further classification of skin alkaloids from neotropical poison frogs (Dendrobatidae), with a general survey of toxic/noxious substances in the amphibia. *Toxicon Off. J. Int. Soc. Toxinology* 25:1023–1095.

Daly JW, Spande TF. 1986. Amphibian alkaloids: chemistry, pharmacology, and biology. *Alkaloids Chem. Biol. Perspect.* 4:1–274.

Damiani MT, Pavarotti M, Leiva N, Lindsay AJ, McCaffrey MW, Colombo MI. 2004. Rab Coupling Protein Associates with Phagosomes and Regulates Recycling from the Phagosomal Compartment. *Traffic* [Internet] 5:785–797. Available from: https://onlinelibrary.wiley.com/doi/abs/10.1111/j.1600-0854.2004.00220.x

Darst CR, Cummings ME. 2006. Predator learning favours mimicry of a less-toxic model in poison frogs. *Nature* 440:208–211.

Deng H, Shang X, Zhu H, Huang N, Wang L, Sun M. 2025. Saxitoxin: A Comprehensive Review of Its History, Structure, Toxicology, Biosynthesis, Detection, and Preventive Implications. *Mar. Drugs* [Internet] 23:277. Available from: https://pmc.ncbi.nlm.nih.gov/articles/PMC12300590/

Drabeck DH, Dean AM, Jansa SA. 2015. Why the honey badger don't care: Convergent evolution of venom-targeted nicotinic acetylcholine receptors in mammals that survive venomous snake bites. *Toxicon* [Internet] 99:68–72. Available from: https://www.sciencedirect.com/science/article/pii/S0041010115000690

Enge A-M, Kaltner F, Gottschalk C, Braeuning A, Hessel-Pras S. 2021. Active Transport of Hepatotoxic Pyrrolizidine Alkaloids in HepaRG Cells. *Int. J. Mol. Sci.* [Internet] 22:3821. Available from: https://www.ncbi.nlm.nih.gov/pmc/articles/PMC8067754/

Engström K, Ameer S, Bernaudat L, Drasch G, Baeuml J, Skerfving S, Bose-O'Reilly S, Broberg K. 2013. Polymorphisms in genes encoding potential mercury transporters and urine mercury concentrations in populations exposed to mercury vapor from gold mining. *Environ. Health Perspect.* 121:85–91.

Feder ME, Hofmann GE. 1999. Heat-shock proteins molecular chaperones and the stress response: Evolutionary and Ecological Physiology. *Annu. Rev. Physiol.* [Internet] 61:243–282. Available from: http://www.ncbi.nlm.nih.gov/pubmed/10099689 http://www.annualreviews.org/doi/10.1146/annurev.physiol.61.1.243

Feldman CR, Brodie ED, Brodie ED, Pfrender ME. 2012. Constraint shapes convergence in tetrodotoxinresistant sodium channels of snakes. *Proc. Natl. Acad. Sci. U. S. A.* [Internet] 109:4556–4561. Available from: www.pnas.org/cgi/doi/10.1073/pnas.1113468109

Feldman CR, Durso AM, Hanifin CT, Pfrender ME, Ducey PK, Stokes AN, Barnett KE, Brodie ED, Brodie ED. 2016. Is there more than one way to skin a newt? Convergent toxin resistance in snakes is not due to a common genetic mechanism. *Heredity* 116:84–91.

Ferrer RP, Zimmer RK. 2012. Community Ecology and the Evolution of Molecules of Keystone Significance. *Biol. Bull.* [Internet] 223:167–177. Available from: https://www.journals.uchicago.edu/doi/10.1086/BBLv223n2p167

Geffeney SL, Fujimoto E, Brodie ED, Brodie ED, Ruben PC. 2005. Evolutionary diversification of TTX-resistant sodium channels in a predator-prey interaction. *Nature* [Internet] 434:759–763. Available from: www.nature.com/nature.

Hague MTJ, Toledo G, Geffeney SL, Hanifin CT, Brodie ED, Brodie ED. 2018. Large-effect mutations generate trade-off between predatory and locomotor ability during arms race coevolution with deadly prey. *Evol. Lett.* [Internet] 2:406–416. Available from: http://doi.wiley.com/10.1002/evl3.76

Halpin CG, Penacchio O, Lovell PG, Cuthill IC, Harris JM, Skelhorn J, Rowe C. 2020. Pattern contrast influences wariness in naïve predators towards aposematic patterns. *Sci. Rep.* [Internet] 10:9246. Available from: https://www.nature.com/articles/s41598-020-65754-y

Halpin CG, Skelhorn J, Rowe C. 2013. Predators' decisions to eat defended prey depend on the size of undefended prey. *Anim. Behav.* [Internet] 85:1315–1321. Available from: https://www.sciencedirect.com/science/article/pii/S0003347213001425

Halpin CG, Skelhorn J, Rowe C. 2014. Increased predation of nutrient-enriched aposematic prey. *Proc. R. Soc. B Biol. Sci.* [Internet] 281. Available from: https://pubmed.ncbi.nlm.nih.gov/24598424/

Han Y-F, Fan X-H, Wang X-J, Sun K, Xue H, Li W-J, Wang Y-B, Chen J-Z, Zhen Y-S, Zhang W-L, et al. 2011. Association of intergenic polymorphism of organic anion transporter 1 and 3 genes with hypertension and blood pressure response to hydrochlorothiazide. *Am. J. Hypertens.* 24:340–346.

Hanifin CT. 2010. The Chemical and Evolutionary Ecology of Tetrodotoxin (TTX) Toxicity in Terrestrial Vertebrates. *Mar. Drugs* [Internet] 8:577–593. Available from: https://pmc.ncbi.nlm.nih.gov/articles/PMC2857372/

Hurlbert SH. 1970. Predator Responses to the Vermilion-Spotted Newt (Notophthalmus viridescens). *J. Herpetol.* [Internet] 4:47–55. Available from: https://www.jstor.org/stable/1562702

Jansa SA, Voss RS. 2011. Adaptive Evolution of the Venom-Targeted vWF Protein in Opossums that Eat Pitvipers. *PLOS ONE* [Internet] 6:1–9. Available from: https://doi.org/10.1371/journal.pone.0020997

Jeckel AM, Draper SJ, Deters BP, Weinberg RB, Tsutsui ND, Tarvin RD. 2026. Ingestion of the potent neurotoxin epibatidine does not compromise locomotion or behavior in the poison frog Epipedobates tricolor. *bioRxiv* [Internet]. Available from: https://www.biorxiv.org/content/early/2026/06/14/2026.06.10.731460

Jones PL, Agrawal AA. 2019. Beyond preference and performance: host plant selection by monarch butterflies, Danaus plexippus. *Oikos* [Internet] 128:1092–1102. Available from: https://onlinelibrary.wiley.com/doi/abs/10.1111/oik.06001

Kawai K, Negoro R, Ichikawa M, Yamashita T, Deguchi S, Harada K, Hirata K, Takayama K, Mizuguchi H. 2020. Establishment of SLC15A1/PEPT1-Knockout Human-Induced Pluripotent Stem Cell Line for Intestinal Drug Absorption Studies. *Mol. Ther. Methods Clin. Dev.* [Internet] 17:49–57. Available from: https://www.cell.com/molecular-therapy-family/methods/abstract/S2329-0501(19)30133-0

Kemp MI, Kemp AC. 1978. Bucorvus and Sagittarius: Two Modes of Terrestrial Predation. In: Proceedings of the Symposium on African Predatory Birds. Pretoria: Northern Transvaal Ornithological Society.

Kim D, Langmead B, Salzberg SL. 2015. HISAT: a fast spliced aligner with low memory requirements. *Nat. Methods* [Internet] 12:357–360. Available from: https://www.nature.com/articles/nmeth.3317

Klure DM, Greenhalgh R, Orr TJ, Shapiro MD, Dearing MD. 2025. Parallel gene expansions drive rapid dietary adaptation in herbivorous woodrats. *Science* [Internet] 387:156–162. Available from: https://www.science.org/doi/10.1126/science.adp7978

Le TNU, Nguyen TQ, Kalailingam P, Nguyen YTK, Sukumar VK, Tan CKH, Tukijan F, Couty L, Hasan Z, Del Gaudio I, et al. 2022. *Mfsd2b* and *Spns2* are essential for maintenance of blood vessels during development and in anaphylactic shock. *Cell Rep.* [Internet] 40:111208. Available from: https://www.sciencedirect.com/science/article/pii/S2211124722010257

Li Y, Jiang Y, Zhang Y, Li N, Yin Q, Liu L, Lv X, Liu Yan, Li A, Fang B, et al. 2021. Abnormal upregulation of cardiovascular disease biomarker PLA2G7 induced by proinflammatory macrophages in COVID-19 patients. *Sci. Rep.* [Internet] 11:6811. Available from: https://www.nature.com/articles/s41598-021-85848-5

Llewellyn LE, Bell PM, Moczydlowski EG. 1997. Phylogenetic survey of soluble saxitoxin-binding activity in pursuit of the function and molecular evolution of saxiphilin, a relative of transferrin. *Proc. Biol. Sci.* 264:891–902.

Llewellyn LE, Doyle J, Negri AP. 1998. A high-throughput, microtiter plate assay for paralytic shellfish poisons using the saxitoxin-specific receptor, saxiphilin. *Anal. Biochem.* 261:51–56.

Love MI, Huber W, Anders S. 2014. Moderated estimation of fold change and dispersion for RNA-seq data with DESeq2. *Genome Biol.* 15:550.

Mackieh R, Abou-Nader R, Wehbe R, Mattei C, Legros C, Fajloun Z, Sabatier JM. 2021. Voltage-Gated Sodium Channels: A Prominent Target of Marine Toxins. *Mar. Drugs* [Internet] 19:562. Available from: https://www.mdpi.com/1660-3397/19/10/562

Mahar J, Lukács GL, Li Y, Hall S, Moczydlowski E. 1991. Pharmacological and biochemical properties of saxiphilin, a soluble saxitoxin-binding protein from the bullfrog (Rana catesbeiana). *Toxicon Off. J. Int. Soc. Toxinology* 29:53–71.

Mappes J, Kokko H, Ojala K, Lindström L. 2014. Seasonal changes in predator community switch the direction of selection for prey defences. *Nat. Commun.* [Internet] 5:5016. Available from: https://www.nature.com/articles/ncomms6016

María Arenas L, Walter D, Stevens M. 2015. Signal honesty and predation risk among a closely related group of aposematic species. *Sci. Rep.* [Internet] 5:11021. Available from: https://www.nature.com/articles/srep11021

Márquez R, Ramírez-Castañeda V, Amézquita A. 2019. Does batrachotoxin autoresistance coevolve with toxicity in Phyllobates poison-dart frogs? *Evolution* [Internet] 73:390–400. Available from: https://onlinelibrary.wiley.com/doi/abs/10.1111/evo.13672

Marshall GAK. 1908. On Diaposematism, with reference to some limitations of the Müllerian Hypothesis of Mimicry. *Trans. R. Entomol. Soc. Lond.* [Internet] 56:93–142. Available from: https://onlinelibrary.wiley.com/doi/abs/10.1111/j.1365-2311.1908.tb02141.x

McGlothlin JW, Chuckalovcak JP, Janes DE, Edwards SV, Feldman CR, Brodie ED, Pfrender ME. 2014. Parallel evolution of tetrodotoxin resistance in three voltage-gated sodium channel genes in the garter snake thamnophis sirtalis. *Mol. Biol. Evol.* 31:2836–2846.

McGlothlin JW, Kobiela ME, Feldman CR, Castoe TA, Geffeney SL, Hanifin CT, Toledo G, Vonk FJ, Richardson MK, Brodie ED, et al. 2016. Historical Contingency in a Multigene Family Facilitates Adaptive Evolution of Toxin Resistance. *Curr. Biol.* 26:1616–1621.

Mohammadi S, Gompert Z, Gonzalez J, Takeuchi H, Mori A, Savitzky AH. 2016. Toxin-resistant isoforms of Na+/K+-ATPase in snakes do not closely track dietary specialization on toads. *Proc. R. Soc. B Biol. Sci.* [Internet] 283:20162111. Available from: https://royalsocietypublishing.org/doi/full/10.1098/rspb.2016.2111

Mohammadi S, McCoy K, Hutchinson D, Gauthier D, Savitzky A. 2013. Independently e volved toad-eating snakes exhibit sexually dimorphic enlargement of adrenal glands. *J. Zool.* 290:237–245.

Mohammadi S, Savitzky AH, Lohr J, Dobler S. 2017. Toad toxin-resistant snake (*Thamnophis elegans*) expresses high levels of mutant Na+/K+-ATPase mRNA in cardiac muscle. *Gene* [Internet] 614:21–25. Available from: https://www.sciencedirect.com/science/article/pii/S0378111917301282

Morabito MA, Moczydlowski E. 1995. Molecular cloning of bullfrog saxiphilin: a unique relative of the transferrin family that binds saxitoxin. *Proc. Natl. Acad. Sci. U. S. A.* 92:6651.

Myers CW, Daly JW, Malkin B. 1978. A dangerously toxic new frog (Phyllobates) used by Emberá Indians of western Colombia, with discussion of blowgun fabrication and dart poisoning. Bulletin of the AMNH ; v. 161, article 2. Available from: http://digitallibrary.amnh.org/handle/2246/1286

Nigam SK. 2015. What do drug transporters really do? *Nat. Rev. Drug Discov.* [Internet] 14:29–44. Available from: https://www.ncbi.nlm.nih.gov/pmc/articles/PMC4750486/

O'Connell LA, O'Connell JD, Paulo JA, Trauger SA, Gygi SP, Murray AW. 2021. Rapid toxin sequestration modifies poison frog physiology. *J. Exp. Biol.* [Internet] 224:jeb230342. Available from: https://pmc.ncbi.nlm.nih.gov/articles/PMC7888741/

Overman LE, Jessup PJ. 1978. Synthetic applications of N-acylamino-1,3-dienes. An efficient stereospecific total synthesis of dl-pumiliotoxin C, and a general entry to cis-decahydroquinoline alkaloids. *J. Am. Chem. Soc.* [Internet] 100:5179–5185. Available from: https://doi.org/10.1021/ja00484a046

Pašukonis A, Loretto M-C. 2020. Predation on the Three-striped poison frog, Ameerega trivitatta (Boulenger 1884; Anura: Dendrobatidae), by Erythrolamprus reginae (Linnaeus 1758; Squamata: Collubridae). Available from: https://www.biotaxa.org/hn/article/view/60062

Pearson KC, Tarvin RD. 2022. A review of chemical defense in harlequin toads (Bufonidae: Atelopus). *Toxicon X* [Internet] 13:100092. Available from: https://www.sciencedirect.com/science/article/pii/S2590171022000029

Penzotti JL, Lipkind G, Fozzard HA, Dudley SC. 2001. Specific Neosaxitoxin Interactions with the Na+ Channel Outer Vestibule Determined by Mutant Cycle Analysis. *Biophys. J.* [Internet] 80:698–706. Available from: https://www.cell.com/biophysj/abstract/S0006-3495(01)76049-3

Perez JC, Haws WC, Hatch CH. 1978. Resistance of woodrats (*Neotoma micropus*) to *Crotalus atrox* venom. *Toxicon* [Internet] 16:198–200. Available from: https://www.sciencedirect.com/science/article/pii/0041010178900399

Pertea G, Pertea M. 2020. GFF Utilities: GffRead and GffCompare. Available from: https://f1000research.com/articles/9-304

Pizzagalli MD, Bensimon A, Superti-Furga G. 2021. A guide to plasma membrane solute carrier proteins. *FEBS J.* [Internet] 288:2784–2835. Available from: https://onlinelibrary.wiley.com/doi/abs/10.1111/febs.15531

Prates I, Antoniazzi MM, Sciani JM, Pimenta DC, Toledo LF, Haddad CFB, Jared C. 2012. Skin glands, poison and mimicry in dendrobatid and leptodactylid amphibians. *J. Morphol.* 273:279–290.

Putri GH, Anders S, Pyl PT, Pimanda JE, Zanini F. 2022. Analysing high-throughput sequencing data in Python with HTSeq 2.0. *Bioinformatics* [Internet] 38:2943–2945. Available from: https://doi.org/10.1093/bioinformatics/btac166

Ramírez-Castañeda V, Tarvin RD, Márquez R. 2026. Snakes (Colubridae: Erythrolamprus) With a Complex Toxic Diet Show Convergent yet Highly Heterogeneous Voltage-gated Sodium Channel Evolution. *Genome Biol. Evol.* [Internet] 18:evag092. Available from: https://doi.org/10.1093/gbe/evag092

Roncalli V, Lenz PH, Cieslak MC, Hartline DK. 2017. Complementary mechanisms for neurotoxin resistance in a copepod. *Sci. Rep.* [Internet] 7:14201. Available from: https://www.nature.com/articles/s41598-017-14545-z

Rowland HM, Fulford AJT, Ruxton GD. 2017. Predator learning differences affect the survival of chemically defended prey. *Anim. Behav.* [Internet] 124:65–74. Available from: https://www.sciencedirect.com/science/article/pii/S0003347216303268

Ruiz-Mazón L, Ramírez-Rico G, Garza M de la. 2024. Lactoferrin: a secret weapon in the war against pathogenic bacteria. *Explor. Drug Sci.* [Internet] 2:734–743. Available from: https://www.explorationpub.com/Journals/eds/Article/100872

Santos JC, Tarvin RD, O'Connell LA. 2016. A Review of Chemical Defense in Poison Frogs (Dendrobatidae): Ecology, Pharmacokinetics, and Autoresistance. In: Schulte BA, Goodwin TE, Ferkin MH, editors. Chemical Signals in Vertebrates 13. Cham: Springer International Publishing. p. 305–337.

Saporito RA, Donnelly MA, Spande TF, Garraffo HM. 2011. A review of chemical ecology in poison frogs. *Chemoecology* [Internet] 22:159–168. Available from: http://link.springer.com/10.1007/s00049-011-0088-0

Scesa P, Nguyen H, Weiss P, Rodriguez AP, Garchow M, Ohlemacher SI, Prappas E, Caplins SA, Bewley CA, Bohnert L, et al. 2024. Defensive polyketides produced by an abundant gastropod are candidate keystone molecules in estuarine ecology. *Sci. Adv.* [Internet] 10:eadp8643. Available from: https://www.science.org/doi/10.1126/sciadv.adp8643

Sherratt TN. 2003. State-dependent risk-taking by predators in systems with defended prey. *Oikos* [Internet] 103:93–100. Available from: https://onlinelibrary.wiley.com/doi/abs/10.1034/j.1600-0706.2003.12576.x

Sherratt TN, Speed MP, Ruxton GD. 2004. Natural selection on unpalatable species imposed by state-dependent foraging behaviour. *J. Theor. Biol.* [Internet] 228:217–226. Available from: https://www.sciencedirect.com/science/article/pii/S0022519304000049

Skelhorn J, Halpin CG, Rowe C. 2016. Learning about aposematic prey. *Behav. Ecol.* 27:955–964.

Skelhorn J, Rowe C. 2007. Predators' Toxin Burdens Influence Their Strategic Decisions to Eat Toxic Prey. *Curr. Biol.* [Internet] 17:1479–1483. Available from: https://www.sciencedirect.com/science/article/pii/S0960982207017885

Smith C, Cranfield J, Allain SJR. 2024. 'Stress and wash' may make great crested Triturus cristatus and smooth newts Lissotriton vulgaris palatable for grey herons Ardea cinerea, with a link to video evidence. *Herpetol. Bull.* [Internet]:33–34. Available from: https://www.thebhs.org/publications/the-herpetological-bulletin/issue-number-170-winter-2024/4226-08-stress-and-wash-may-make-great-crested-i-triturus-cristatus-i-and-smooth-newts-lissotriton-vulgaris-palatable-for-grey-herons-i-ardea-cinerea-i-with-a-link-to-video-evidence

Speed MP. 1993. Muellerian mimicry and the psychology of predation. *Anim. Behav.* 45:571–580.

Spolaore B, Fernández J, Lomonte B, Massimino ML, Tonello F. 2019. Enzymatic labelling of snake venom phospholipase A2 toxins. *Toxicon* [Internet] 170:99–107. Available from: https://www.sciencedirect.com/science/article/pii/S0041010119304696

Tarvin RD, Borghese CM, Sachs W, Santos JC, Lu Y, O'Connell LA, Cannatella DC, Harris RA, Zakon HH. 2017. Interacting amino acid replacements allow poison frogs to evolve epibatidine resistance. *Science* 357:1261–1266.

Tarvin RD, Coleman JL, Donoso DA, Betancourth-Cundar M, López-Hervas K, Gleason KS, Sanders JR, Smith JM, Ron SR, Santos JC, et al. 2024. Passive accumulation of alkaloids in inconspicuously colored frogs refines the evolutionary paradigm of acquired chemical defenses.Joo Y, Rasmann S, editors. *eLife* [Internet] 13:RP100011. Available from: https://doi.org/10.7554/eLife.100011

Tarvin RD, Pearson KC, Douglas TE, Ramírez-Castañeda V, Navarrete MJ. 2023. The Diverse Mechanisms that Animals Use to Resist Toxins. *Annu. Rev. Ecol. Evol. Syst.* [Internet] 54:283–306. Available from: https://doi.org/10.1146/annurev-ecolsys-102320-102117

Tarvin RD, Santos JC, O'Connell LA, Zakon HH, Cannatella DC. 2016. Convergent substitutions in a sodium channel suggest multiple origins of toxin resistance in poison frogs. *Mol. Biol. Evol.* [Internet] 33:1068–1081. Available from: http://www.ncbi.nlm.nih.gov/pubmed/26782998 https://academic.oup.com/mbe/article-lookup/doi/10.1093/molbev/msv350

Terlau H, Heinemann SH, Stühmer W, Pusch M, Conti F, Imoto K, Numa S. 1991. Mapping the site of block by tetrodotoxin and saxitoxin of sodium channel II. *FEBS Lett.* [Internet] 293:93–96. Available from: https://www.sciencedirect.com/science/article/pii/0014579391811596

van Thiel J, Khan MA, Wouters RM, Harris RJ, Casewell NR, Fry BG, Kini RM, Mackessy SP, Vonk FJ, Wüster W, et al. 2022. Convergent evolution of toxin resistance in animals. *Biol. Rev.* [Internet] 97:1823–1843. Available from: https://onlinelibrary.wiley.com/doi/abs/10.1111/brv.12865

Toledo G, Hanifin C, Geffeney S, Brodie ED. 2016. Chapter Four - Convergent Evolution of Tetrodotoxin-Resistant Sodium Channels in Predators and Prey. In: French RJ, Noskov SY, editors. Na Channels from Phyla to Function. Vol. 78. Current Topics in Membranes. Academic Press. p. 87–113. Available from: https://www.sciencedirect.com/science/article/pii/S1063582316300138

Tortorella S, Karagiannis TC. 2014. Transferrin Receptor-Mediated Endocytosis: A Useful Target for Cancer Therapy. *J. Membr. Biol.* [Internet] 247:291–307. Available from: https://link.springer.com/article/10.1007/s00232-014-9637-0

Ujvari B, Casewell NR, Sunagar K, Arbuckle K, Wüster W, Lo N, O'Meally D, Beckmann C, King GF, Deplazes E, et al. 2015. Widespread convergence in toxin resistance by predictable molecular evolution. *Proc. Natl. Acad. Sci.* [Internet] 112:11911–11916. Available from: https://www.pnas.org/doi/full/10.1073/pnas.1511706112

Underhill R. 2015. Mayne Island, B.C. Wetlands and Amphibian Habitats. Mayne Island Conservancy Society

Vaelli PM, Theis KR, Williams JE, O'Connell LA, Foster JA, Eisthen HL. 2020. The skin microbiome facilitates adaptive tetrodotoxin production in poisonous newts.Baldwin IT, Robert CA, Robert CA, González Montoya MC, editors. *eLife* [Internet] 9:e53898. Available from: https://doi.org/10.7554/eLife.53898

Vandendriessche T, Abdel-Mottaleb Y, Maertens C, Cuypers E, Sudau A, Nubbemeyer U, Mebs D, Tytgat J. 2008. Modulation of voltage-gated Na+ and K+ channels by pumiliotoxin 251D: A "joint venture" alkaloid from arthropods and amphibians. *Toxicon* 51:334–344.

Voss RS, Jansa SA. 2012. Snake-venom resistance as a mammalian trophic adaptation: lessons from didelphid marsupials. *Biol. Rev. Camb. Philos. Soc.* 87:822–837.

Vu TM, Ishizu A-N, Foo JC, Toh XR, Zhang F, Whee DM, Torta F, Cazenave-Gassiot A, Matsumura T, Kim S, et al. 2017. Mfsd2b is essential for the sphingosine-1-phosphate export in erythrocytes and platelets. *Nature* [Internet] 550:524–528. Available from: https://www.nature.com/articles/nature24053

Waizenegger J, Glück J, Henricsson M, Luckert C, Braeuning A, Hessel-Pras S. 2021. Pyrrolizidine Alkaloids Disturb Bile Acid Homeostasis in the Human Hepatoma Cell Line HepaRG. *Foods* [Internet] 10:161. Available from: https://www.ncbi.nlm.nih.gov/pmc/articles/PMC7828834/

Wang S-Y, Wang GK. 2017. Single rat muscle Na+ channel mutation confers batrachotoxin autoresistance found in poison-dart frog Phyllobates terribilis. *Proc. Natl. Acad. Sci. U. S. A.* 114:10491–10496.

Wei Y, Mao H, Liu Q, Fang W, Zhang T, Xu Y, Zhang W, Chen B, Zheng Y, Hu X. 2025. Lipid metabolism and microbial regulation analyses provide insights into the energy-saving strategies of hibernating snakes. *Commun. Biol.* [Internet] 8:1–13. Available from: https://www.nature.com/articles/s42003-025-07493-2

Wiese M, D'Agostino PM, Mihali TK, Moffitt MC, Neilan BA. 2010. Neurotoxic Alkaloids: Saxitoxin and Its Analogs. *Mar. Drugs* [Internet] 8:2185–2211. Available from: https://www.mdpi.com/1660-3397/8/7/2185

Williams BL, Hanifin CT, Brodie ED, III EDB. 2010. Tetrodotoxin affects survival probability of rough-skinned newts (Taricha granulosa) faced with TTX-resistant garter snake predators (Thamnophis sirtalis). *Chemoecology* [Internet] 20:285–290. Available from: http://link.springer.com/10.1007/s00049-010-0057-z

Yeager J, Viteri Chancusi PA, Perez-Castillo Y, Armijos-Jaramillo V, Tejera E. 2024. Modeling defensive functions of alkaloids within diverse chemical portfolios. *Evol. Ecol.* [Internet] 38:727–745. Available from: https://doi.org/10.1007/s10682-023-10252-6

Yee SW, Nguyen AN, Brown C, Savic RM, Zhang Y, Castro RA, Cropp CD, Choi JH, Singh D, Tahara H, et al. 2013. Reduced renal clearance of cefotaxime in asians with a low-frequency polymorphism of OAT3 (SLC22A8). *J. Pharm. Sci.* 102:3451–3457.

Yen T-J, Lolicato M, Thomas-Tran R, Du Bois J, Minor DL. 2019. Structure of the saxiphilin:saxitoxin (STX) complex reveals a convergent molecular recognition strategy for paralytic toxins. *Sci. Adv.* [Internet] 5:eaax2650. Available from: https://www.science.org/doi/10.1126/sciadv.aax2650

Yotsu-Yamashita M, Sugimoto A, Terakawa T, Shoji Y, Miyazawa T, Yasumoto T. 2001. Purification, characterization, and cDNA cloning of a novel soluble saxitoxin and tetrodotoxin binding protein from plasma of the puffer fish, Fugu pardalis. *Eur. J. Biochem.* 268:5937–5946.

Zakrzewska S, Nixon SA, Chen Z, Hajare HS, Park ER, Mulcahy JV, Arlinghaus KM, Neu E, Konovalov K, Provasi D, et al. 2025. Structural basis for saxitoxin congener binding and neutralization by anuran saxiphilins. *Nat. Commun.* [Internet] 16:3885. Available from: https://www.nature.com/articles/s41467-025-58903-2

Figures and Tables

A

B

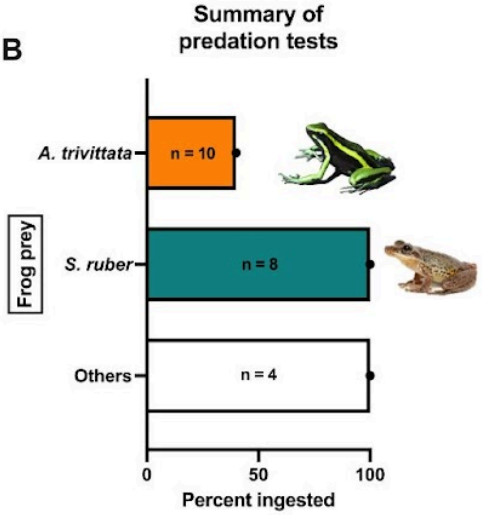
Summary of predation tests
Frog prey
A. trivittata
n = 10
S. ruber
n = 8
Others
n = 4
0
50
100
Percent ingested

C

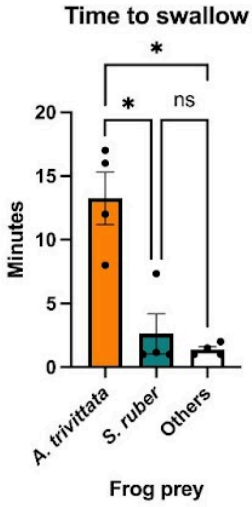
Time to swallow
*
*
ns
Minutes
20
15
10
5
0
A. trivittata
S. ruber
Others
Frog prey

D

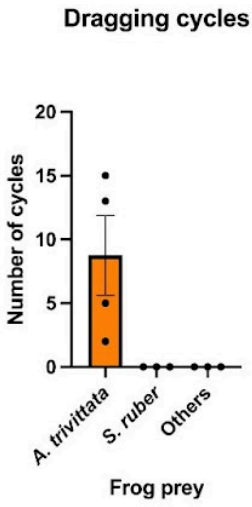
Dragging cycles
Number of cycles
20
15
10
5
0
A. trivittata
S. ruber
Others
Frog prey

E

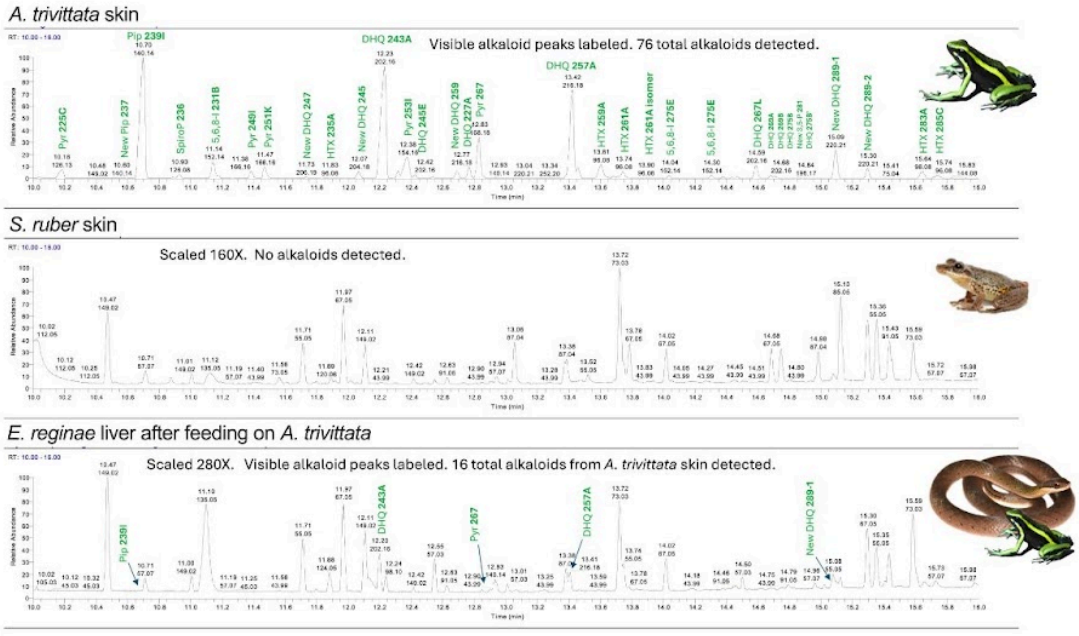
A. trivittata skin
Visible alkaloid peaks labeled. 76 total alkaloids detected.
S. ruber skin
Scaled 160X. No alkaloids detected.
E. reginae liver after feeding on A. trivittata
Scaled 280X. Visible alkaloid peaks labeled. 16 total alkaloids from A. trivittata skin detected.

Figure 1. *E. reginae* presented longer swallowing times and a dragging behavior when feeding on the poisonous frog *Ameerega trivittata*. (**A**) *Erythrolamprus reginae* feeding on a three-striped poison frog (*A. trivittata*), photographed by Leonardo Castañeda. (**B**) Summary of predation trials and ingestion percentages. *A. trivittata* (high alkaloid content) was offered to *E. reginae* 10 times, of which only four frogs were consumed. One snake died after *A. trivittata* ingestion. *S. ruber* (no alkaloids) was offered eight times, and all were consumed, as well as four individuals of other frog species (1 *Dendropsophus* sp., 1 *Leptodactulus* sp., 1 *Rhinella margaritifera* and 1 *Sphaenorynchus lacteus*) that were offered. (**C**) Comparison of swallowing time between *E. reginae* feeding on *A. trivittata*, *S. ruber*, and other species revealed a significant difference (Kruskal-Wallis test; *, $P \leq 0.05$). (**D**) Analysis of drag cycle behavior during predation revealed that this behavior was exhibited only when feeding on *A. trivittata*. In contrast, no such behavior was observed when feeding on *S. ruber* or other species. (**E**) GC-MS example result from an *A. trivittata* skin, *S. ruber* skin, and *E. reginae* liver after feeding on *A. trivittata*.

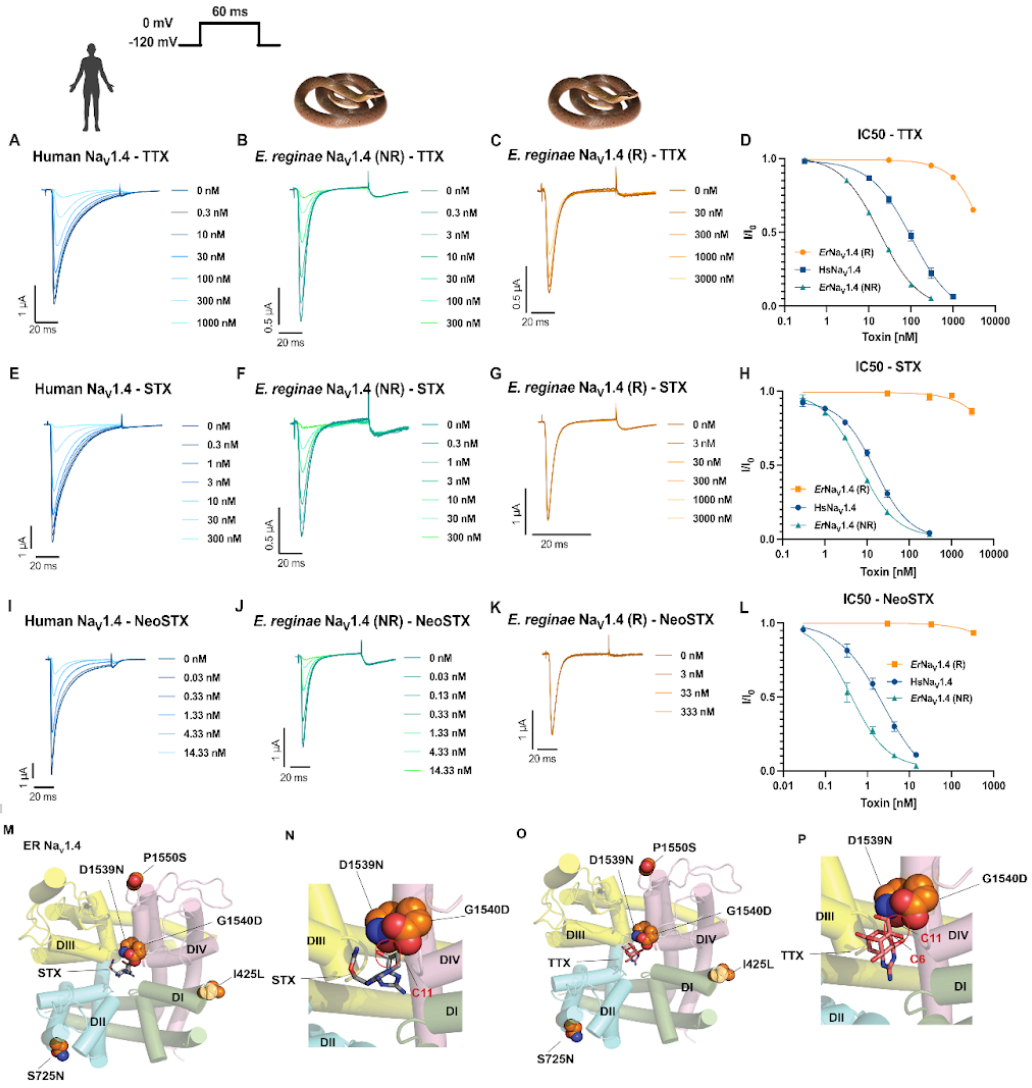
0 mV
-120 mV
60 ms
A
Human Na$_V$1.4 - TTX
0 nM
0.3 nM
10 nM
30 nM
100 nM
300 nM
1000 nM
B
E. reginae Na$_V$1.4 (NR) - TTX
0 nM
0.3 nM
3 nM
10 nM
30 nM
100 nM
300 nM
C
E. reginae Na$_V$1.4 (R) - TTX
0 nM
30 nM
300 nM
1000 nM
3000 nM
D
IC50 - TTX
ErNa$_V$1.4 (R)
HsNa$_V$1.4
ErNa$_V$1.4 (NR)
I/I$_0$
Toxin [nM]
E
Human Na$_V$1.4 - STX
0 nM
0.3 nM
1 nM
3 nM
10 nM
30 nM
300 nM
F
E. reginae Na$_V$1.4 (NR) - STX
0 nM
0.3 nM
1 nM
3 nM
10 nM
30 nM
300 nM
G
E. reginae Na$_V$1.4 (R) - STX
0 nM
3 nM
30 nM
300 nM
1000 nM
3000 nM
H
IC50 - STX
ErNa$_V$1.4 (R)
HsNa$_V$1.4
ErNa$_V$1.4 (NR)
I/I$_0$
Toxin [nM]
I
Human Na$_V$1.4 - NeoSTX
0 nM
0.03 nM
0.33 nM
1.33 nM
4.33 nM
14.33 nM
J
E. reginae Na$_V$1.4 (NR) - NeoSTX
0 nM
0.03 nM
0.13 nM
0.33 nM
1.33 nM
4.33 nM
14.33 nM
K
E. reginae Na$_V$1.4 (R) - NeoSTX
0 nM
3 nM
33 nM
333 nM
L
IC50 - NeoSTX
ErNa$_V$1.4 (R)
HsNa$_V$1.4
ErNa$_V$1.4 (NR)
I/I$_0$
Toxin [nM]
M
ER Na$_V$1.4
D1539N
P1550S
G1540D
DIII
DIV
STX
I425L
DI
DII
S725N
N
D1539N
G1540D
DIII
DIV
STX
C11
DI
DII
O
D1539N
P1550S
G1540D
DIII
DIV
TTX
I425L
DI
DII
S725N
P
D1539N
G1540D
DIII
C11
DIV
TTX
C6
DI
DII

Figure 2. Amino acid substitutions in *Er*Na_V1.4-R confer high resistance to the neurotoxins TTX, STX, and neoSTX. Exemplar recordings for Human Na_V1.4 (*Hs*Na_V1.4, blue), *E. reginae* Na_V1.4 non-resistant variant (*Er*Na_V1.4-NR, green), and *E. reginae* Na_V1.4 resistant variant (*Er*Na_V1.4-R in orange) expressed in oocytes were exposed to increasing concentrations of TTX (**A, B, C**), STX (**E, F, G**) and neoSTX (**I, J, K**). Concentration-response curves were subsequently plotted for each Na_V channel for TTX, STX, and neoSTX (**D, H, L**; respectively; for values, see Table S2). Each point represents mean normalized current with standard deviation (n = 6). Note the different toxin concentrations used for *Er*Na_V1.4-R (**C, G,** and **K**) compared to other graphs. Structural interactions of STX (**M, N**) and TTX (**O, P**) with a model of the *Er*Na_V1.4-R variant. Residues shown in space-filling representation highlight the five amino acid substitutions at functionally relevant sites that differentiate *Er*Na_V1.4-R and *Er*Na_V1.4-NR. Among these, only D1539N and G1540D appear to interact directly with the guanidinium toxins. Residue numbers correspond to the position in *Hs*Na_V1.4.

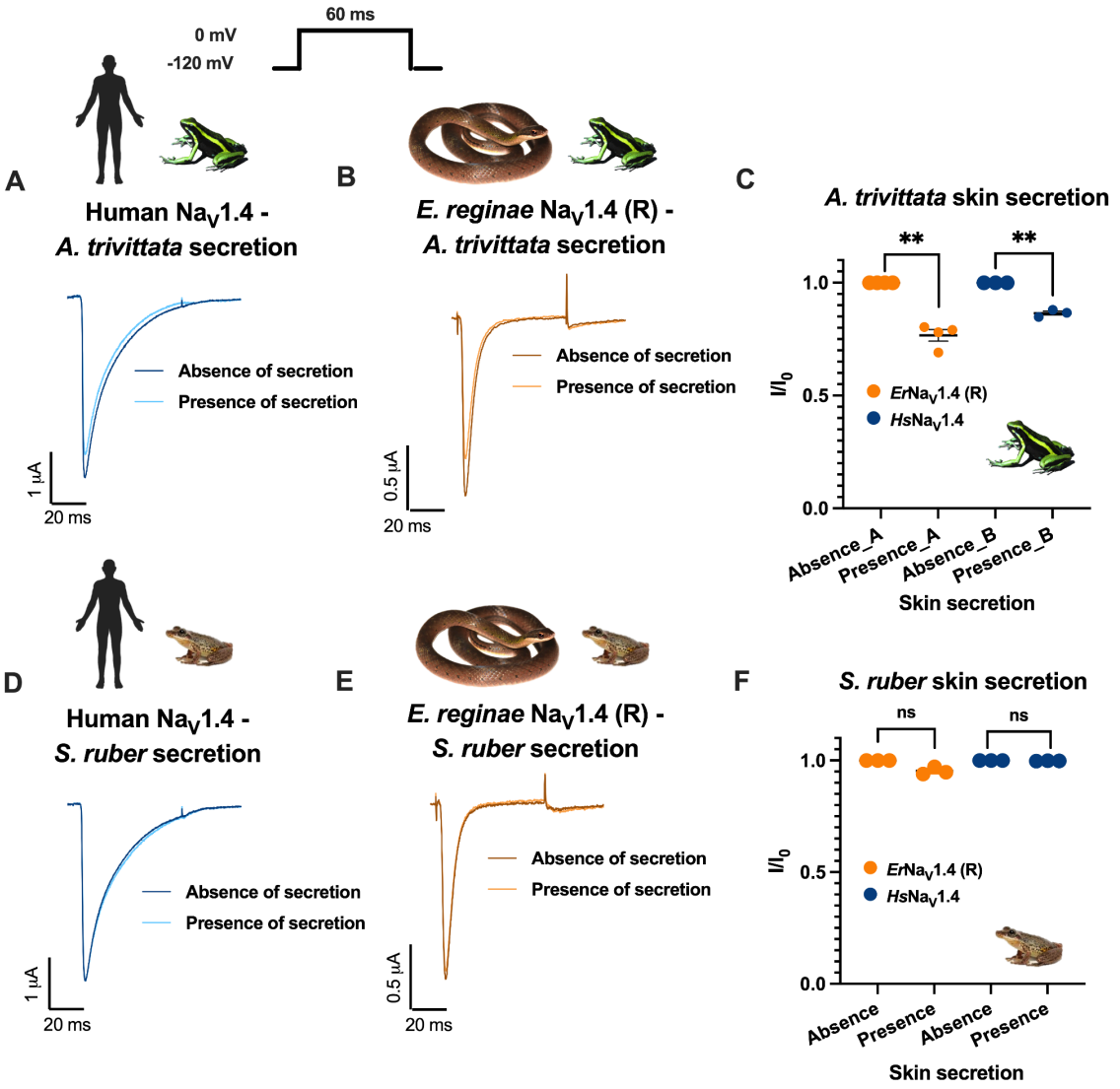

Figure 3. *Er*Na$_V$1.4-R is sensitive to the *A. trivittata* poison frog skin secretions. Exemplar current recordings for *Hs*Na$_V$1.4 (blue) and *Er*Na$_V$1.4-R (orange) expressed in *X. laevis* oocytes and exposed to 1:1000 dilution of reconstituted skin secretions from *A. trivittata* (**A**, **B**) or *S. ruber* (**D, E**). Comparison of sodium current reduction in the presence or absence of *A. trivittata* (**C**) and *S. ruber* (**F**) skin secretions. Statistical significance was assessed using a one-sided T-test, with p-values provided for the corresponding comparisons. P-values are shown in the graph as (ns) $P > 0.01$; (*) $P \leq 0.01$; (**) $P \leq 0.01$; (***) $P \leq 0.001$.

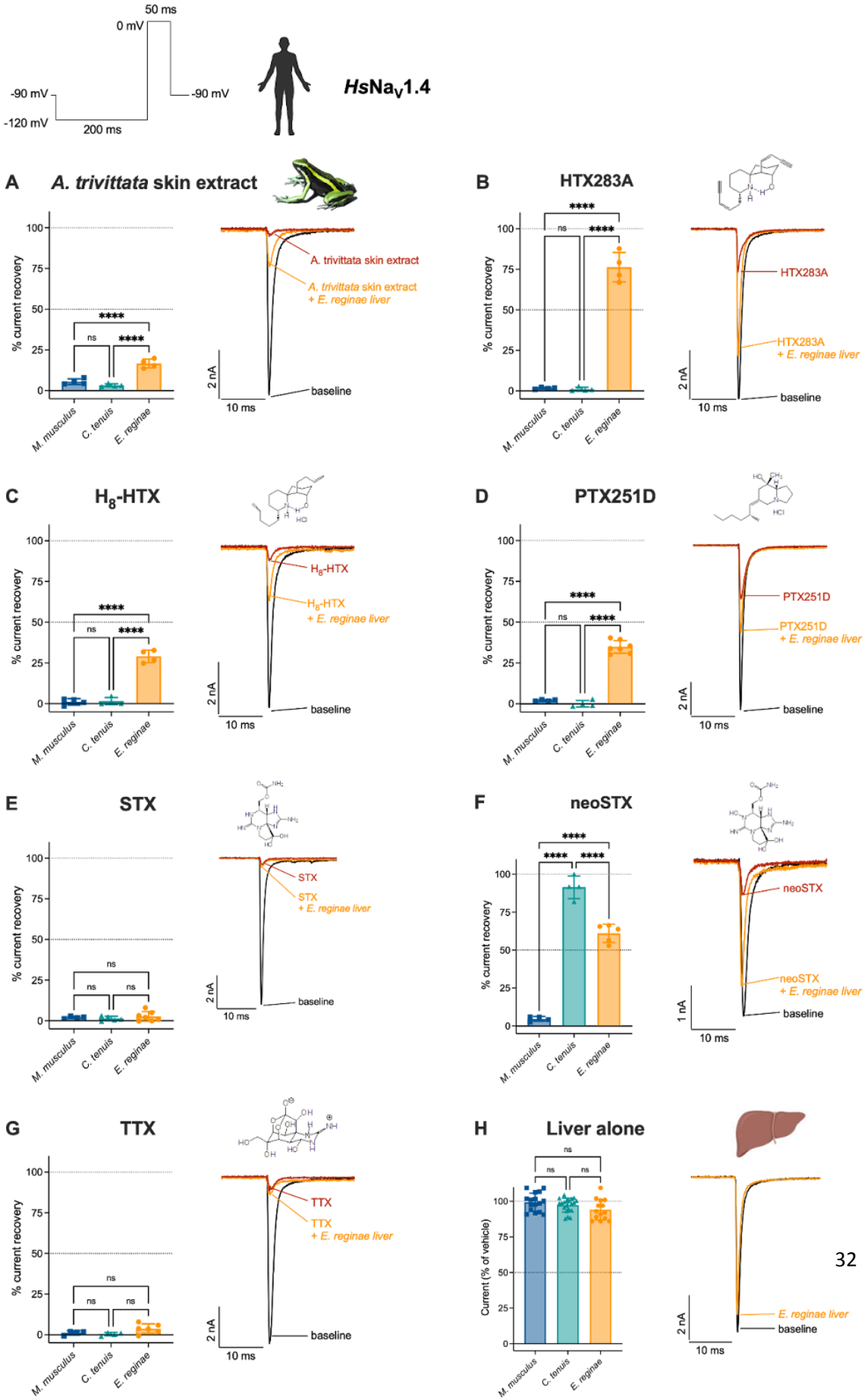
50 ms
0 mV
-90 mV
-120 mV
200 ms
-90 mV
HsNaV1.4
A
A. trivittata skin extract
% current recovery
100
75
50
25
0
****
ns
****
M. musculus
C. tenuis
E. reginae
A. trivittata skin extract
A. trivittata skin extract
+ E. reginae liver
2 nA
10 ms
baseline
B
HTX283A
****
ns
****
HTX283A
HTX283A
+ E. reginae liver
C
H8-HTX
H8-HTX
H8-HTX
+ E. reginae liver
D
PTX251D
PTX251D
PTX251D
+ E. reginae liver
E
STX
STX
STX
+ E. reginae liver
F
neoSTX
neoSTX
neoSTX
+ E. reginae liver
1 nA
G
TTX
TTX
TTX
+ E. reginae liver
H
Liver alone
Current (% of vehicle)
E. reginae liver
baseline

Figure 4. *E. reginae* liver extract mitigates dendrobatid toxin and neoSTX block of *Hs*Na_V1.4, providing evidence of liver proteins involved in detoxification. Concentrations used: (**A**), *A. trivittata* skin extract, diluted 1:200; (**B**), HTX **283A**, 500 μM; (**C**), H_8-HTX, 250 μM; (**D**), PTX **251D**, 500 μM; (**E**), STX, 100 nM; (**F**), neoSTX, 1.5 nM; (**G**), TTX, 300 nM; (**H**), liver extract alone, 0.2 mg/mL. For all toxins and extracts, exemplar whole-cell patch-clamp recordings of *Hs*Na_V1.4 expressed in CHO cells are plotted in the absence of toxin (baseline, black), presence of toxin alone (maroon), and toxin mixed with *E. reginae* liver extract (orange). Current recovery with liver-treated toxin relative to baseline and toxin alone, for *E. reginae* liver (orange), *C. tenuis* liver (teal), and mouse liver (blue). Each point represents a single cell (n = minimum of 4 cells) and error bars represent standard deviation. Asterisks represent statistically significant differences in toxin current recovery between extracts ($P < 0.0001$, one-way ANOVA with Tukey's post hoc test).

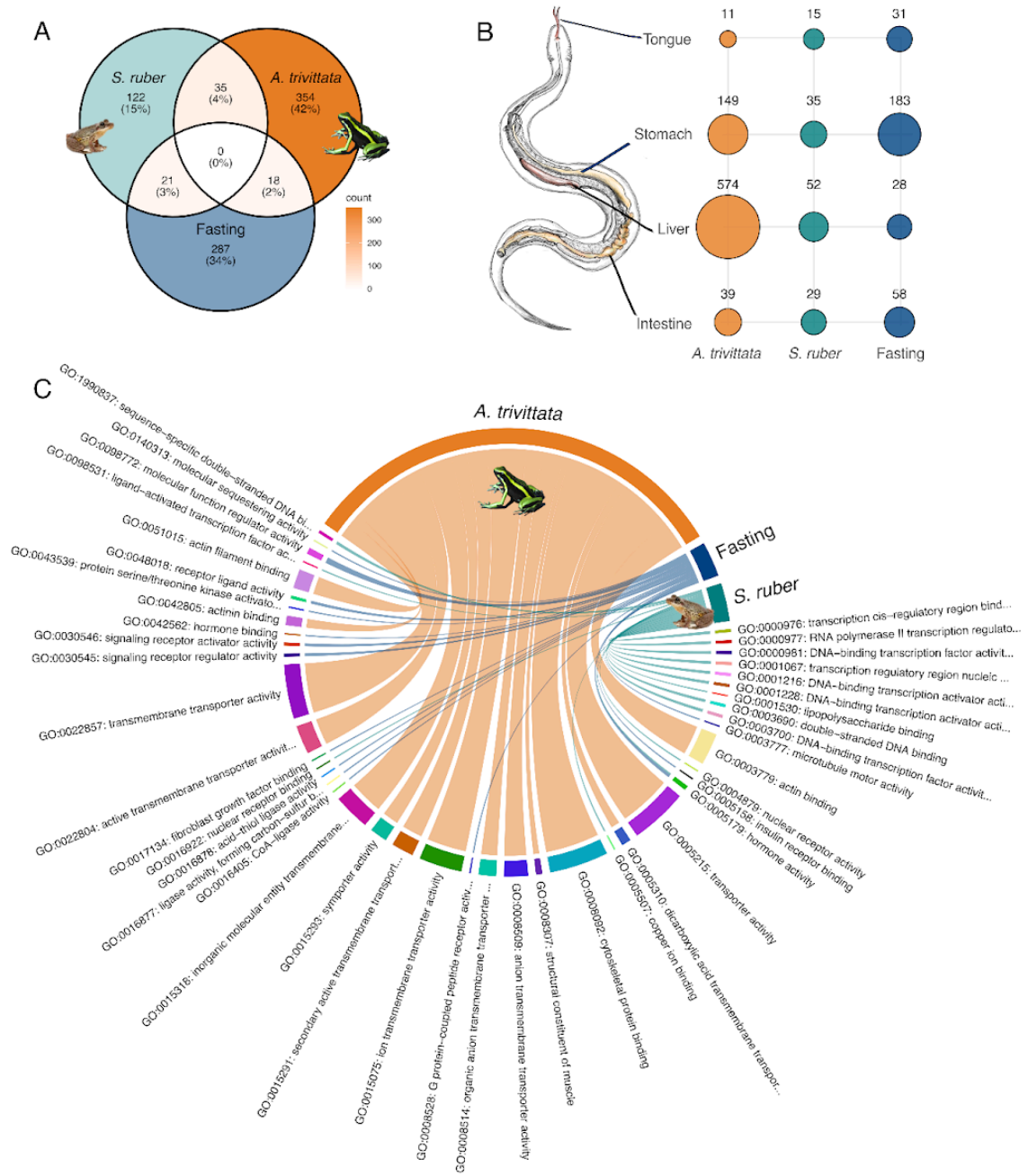
A
S. ruber
122
(15%)
A. trivittata
354
(42%)
Fasting
287
(34%)
35
(4%)
0
(0%)
21
(3%)
18
(2%)
count
300
200
100
0
B
Tongue
Stomach
Liver
Intestine
11
15
31
149
35
183
574
52
28
39
29
58
A. trivittata
S. ruber
Fasting
C
A. trivittata
Fasting
S. ruber
GO:1990837: sequence-specific double-stranded DNA bi...
GO:0140313: molecular sequestering activity
GO:0098772: molecular function regulator activity
GO:0098531: ligand-activated transcription factor ac...
GO:0051015: actin filament binding
GO:0048018: receptor ligand activity
GO:0043539: protein serine/threonine kinase activato...
GO:0042805: actinin binding
GO:0042562: hormone binding
GO:0030546: signaling receptor activator activity
GO:0030545: signaling receptor regulator activity
GO:0022857: transmembrane transporter activity
GO:0022804: active transmembrane transporter activit...
GO:0017134: fibroblast growth factor binding
GO:0016922: nuclear receptor binding
GO:0016878: acid-thiol ligase activity
GO:0016877: ligase activity, forming carbon-sulfur b...
GO:0016405: CoA-ligase activity
GO:0015318: inorganic molecular entity transmembrane...
GO:0015293: symporter activity
GO:0015291: secondary active transmembrane transport...
GO:0015075: ion transmembrane transporter activity
GO:0008528: G protein-coupled peptide receptor activ...
GO:0008514: organic anion transmembrane transporter ...
GO:0008509: anion transmembrane transporter activity
GO:0008307: structural constituent of muscle
GO:0008092: cytoskeletal protein binding
GO:0005507: copper ion binding
GO:0005310: dicarboxylic acid transmembrane transpor...
GO:0005215: transporter activity
GO:0005179: hormone activity
GO:0005158: insulin receptor binding
GO:0004879: nuclear receptor activity
GO:0003779: actin binding
GO:0003777: microtubule motor activity
GO:0003700: DNA-binding transcription factor activit...
GO:0003690: double-stranded DNA binding
GO:0001530: lipopolysaccharide binding
GO:0001228: DNA-binding transcription activator acti...
GO:0001216: DNA-binding transcription activator acti...
GO:0001067: transcription regulatory region nucleic ...
GO:0000981: DNA-binding transcription factor activit...
GO:0000977: RNA polymerase II transcription regulato...
GO:0000976: transcription cis-regulatory region bind...

Figure 5. Consumption of *A. trivittata* changes liver gene expression in *E. reginae* more than in other conditions and induces high expression of transporter genes. (**A**) Venn diagram showing the overlap of upregulated protein-coding transcripts across three conditions after differential expression analysis between fasting vs. *A trivittata*, fasting vs. *S. ruber*, and *S. ruber* vs. *A. trivittata* of the combined digestive system tissues (tongue, stomach, liver, and intestine). (**B**) Number of upregulated protein-coding transcripts in each digestive tissue after differential expression analysis between fasting vs. *A trivittata*, fasting vs. *S. ruber*, and *S. ruber* vs. *A. trivittata*. Snake diagram was drawn by Bernardo Moreno Peniche. (**C**) Circular plot representing the upregulated liver Gene Ontology (GO) enrichment analysis (molecular function category) using topGO in *E. reginae* across the three conditions. Each segment represents a GO term. The width of each segment corresponds to the "Significant" value, indicating the number of upregulated genes associated with each GO term.

Supporting Information for

Toxin resistance mechanisms span biological scales in the Royal Ground Snake *Erythrolamprus reginae*.

This PDF file includes:

Figures S1 to S8
Tables S1 to S3
SI References

Other Supplementary Materials for this manuscript include the following:

Movies S1 to S2
Datasets S1 to S8

Figures

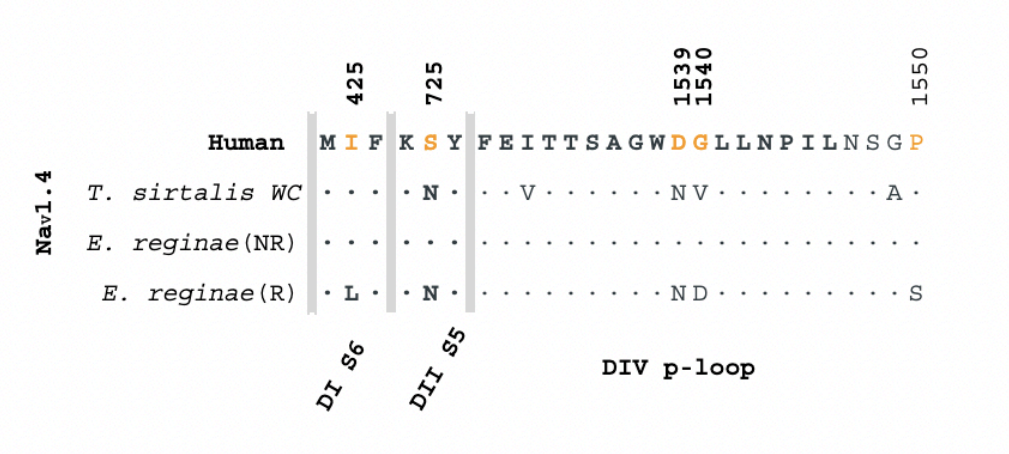

Fig. S1. The set of amino acid differences between *E. reginae* non-resistant and resistant $Na_V1.4$ variants introduced the cloning vector.

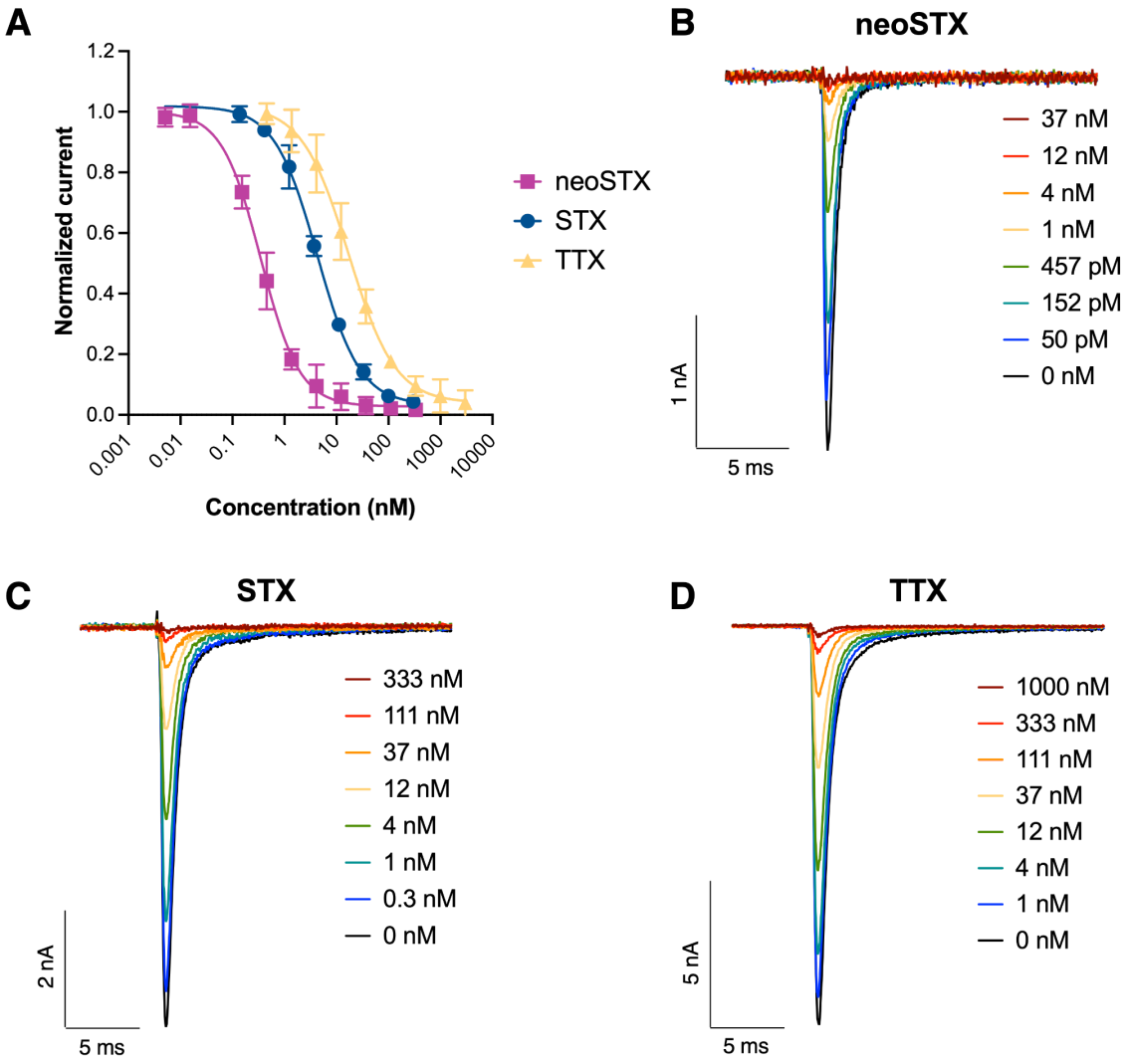

Fig. S2. Whole-cell patch-clamp recordings of *Hs*Na$_V$1.4 responses to guanidinium toxins. (**A**) Concentration-response curves to neoSTX (purple, squares), STX (blue, circles) and TTX (yellow, triangles). Each point represents the mean with standard deviation, n = 5–6 cells. (**B–D**) Exemplar whole-cell patch-clamp recordings for increasing concentrations of toxins for neoSTX (**B**), STX (**C**), and TTX (**D**).

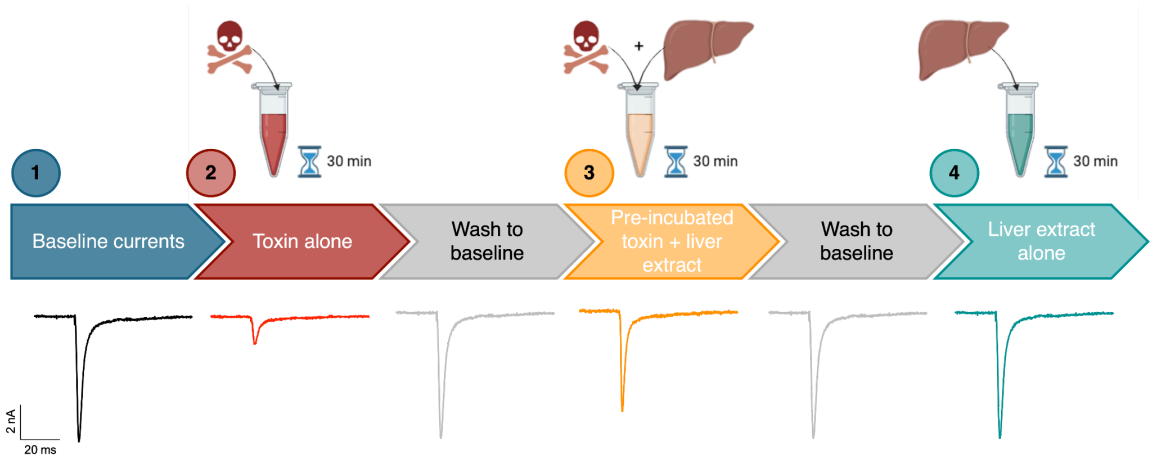

Fig. S3. Schematic for liver extract functional toxin neutralization assay with example *Hs*Na$_V$1.4 currents. The capacity for liver protein extracts from different organisms to inhibit the toxin block of *Hs*Na$_V$1.4 were measured by planar patch-clamp assay using a QPatch Compact II (Sophion Bioscience). Cells were sequentially exposed to four different conditions, with wash steps between: **1. Baseline currents** in ECS (blue), with no toxin or liver extract. **2. Toxin alone** (red), TTX, STX, neoSTX, PTX251D, H8-HTX, HTX283A, and *A. trivittata* skin secretion were diluted in ECS to concentrations sufficient to inhibit *Hs*Na$_V$1.4 currents by at least 60% and were pre-incubated for 30 minutes before addition to cells. **3. Toxin:liver extract mixture** (yellow), toxins from section 2. were pre-incubated for 30 minutes at room temperature with liver extracts (final concentration 0.2 mg/mL) from *E. reginae*, *C. tenuis* (a control species of Colubrid snake from California, USA, with no known exposure to dendrobatid toxins), and mouse liver. If the toxin block observed in section 2. was reduced in the presence of a liver extract, we inferred that the extract contained a detoxifying or toxin-binding protein. **4. Liver alone** (teal)**,** liver extracts alone (final concentration 0.2 mg/mL) were incubated for 30 minutes at room temperature and added to the cells. If the liver extract alone affected sodium channel function, it would indicate intrinsic toxicity to *Hs*Na$_V$1.4. Figure was partially generated using https://Biorender.com.

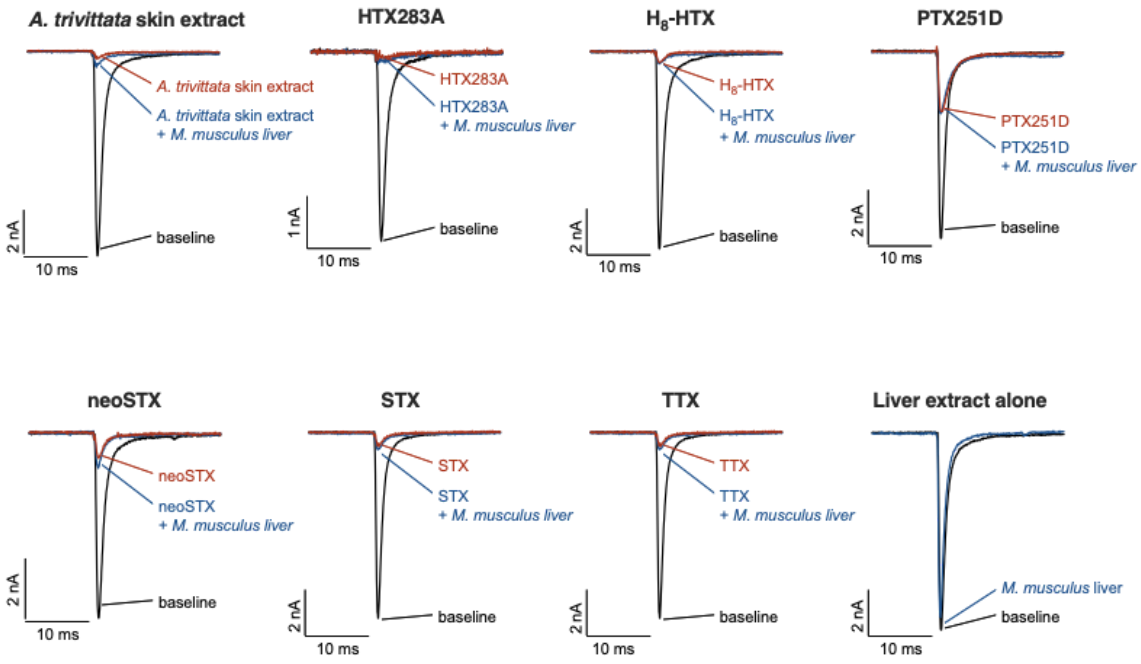

Fig. S4. Mouse liver extract does not affect toxin block of *Hs*NaV1.4. Exemplar whole-cell patch-clamp recordings of *Hs*Na_V1.4 expressed in CHO cells in the absence of toxin (baseline, black), presence of toxin alone (maroon) and toxin mixed with *M. musculus* liver extract (blue). Toxin concentrations used: *A. trivittata* skin extract diluted 1:200; HTX283A, 500 µM; H_8-HTX, 250 µM; PTX251D, 500 µM; neoSTX, 1.5 nM; STX, 100 nM; TTX, 300 nM. Final liver concentration was 0.2 mg/mL.

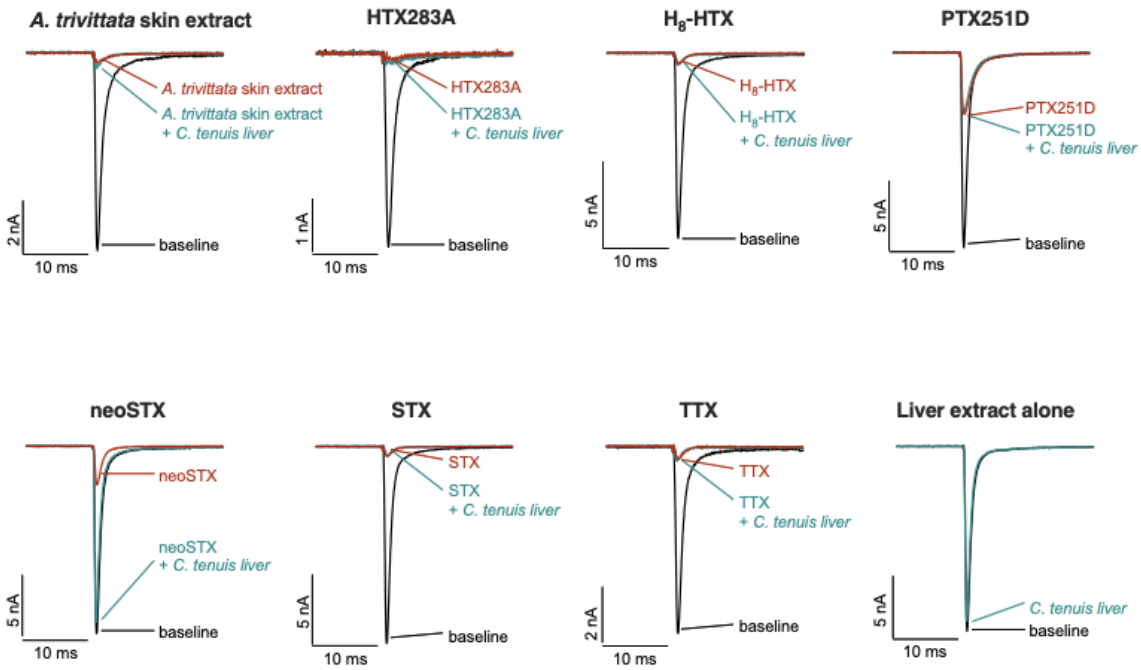

Fig. S5. *C. tenuis* liver extract ameliorates neoSTX block of *Hs*Na_V1.4, but does not affect STX, TTX or dendrobatid toxin block. Exemplar whole-cell patch-clamp recordings of *Hs*Na_V1.4 expressed in CHO cells in the absence of toxin (baseline, black), presence of toxin alone (maroon), and toxin mixed with *C. tenuis* liver extract (teal). Toxin concentrations used: *A. trivittata* skin extract diluted 1:200; HTX283A, 500 µM; H_8-HTX, 250 µM; PTX251D, 500 µM; neoSTX, 1.5 nM; STX, 100 nM; TTX, 300 nM. Final liver concentration was 0.2 mg/mL.

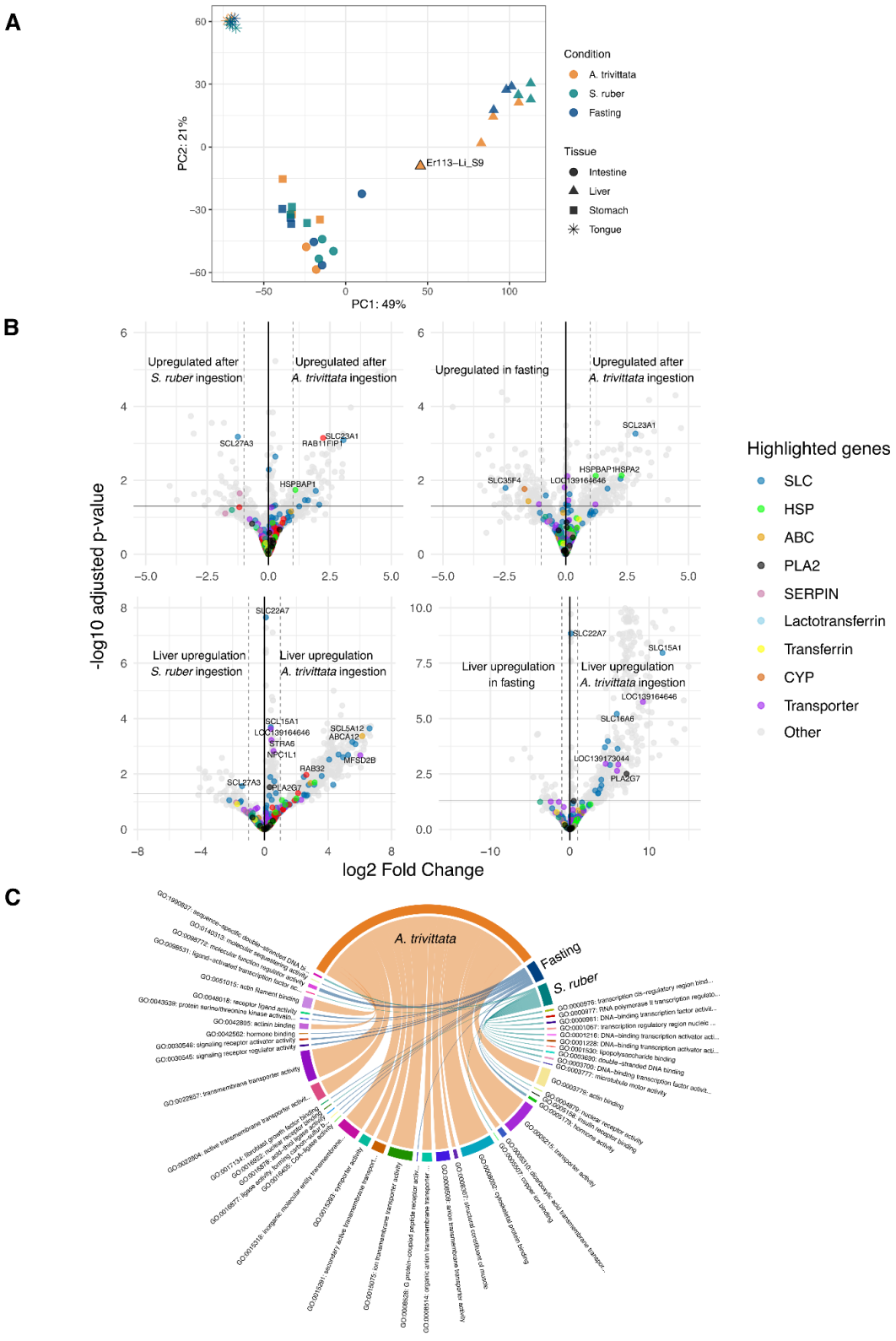

Fig. S6. Transcriptomic responses of *E. reginae* after consumption of *A. trivittata*, *S. ruber*, or under fasting conditions. (**A**) Principal Component Analysis (PCA) of variance-stabilized transformed (VST)

transcriptomic data from the DESeq2 package (1) across four tissues (tongue, liver, stomach, and intestine) under three dietary conditions: consumption of *A. trivittata*, *S. ruber*, or fasting. The sample Er113_Li_S9 correspond to the snake that died after *A. trivittata* ingestion (see Table S2). (**B**) Volcano plots showing differentially expressed genes across all tissues and in liver tissue for two pairwise comparisons: fasting vs. *A. trivittata* and *S. ruber* vs. *A. trivittata*. Gene families previously associated with toxin resistance were highlighted, including solute carriers (SLC), phospholipases (PLA2), cytochrome P450s (CYP), serpins (SERPIN), ATP-binding cassette transporters (ABC), heat shock proteins (HSP), Rab GTPases (RAB), cholinesterase-like genes, transferrin-related genes, lactotransferases and other *E. reginae* genes annotated in NCBI as transporters. (**C**) Circular plot showing liver-specific Gene Ontology (GO) enrichment analysis for upregulated genes under the cellular component category, using topGO (2). Each segment represents a GO term, with segment width corresponding to the number of upregulated genes annotated with that term ("Significant" value).

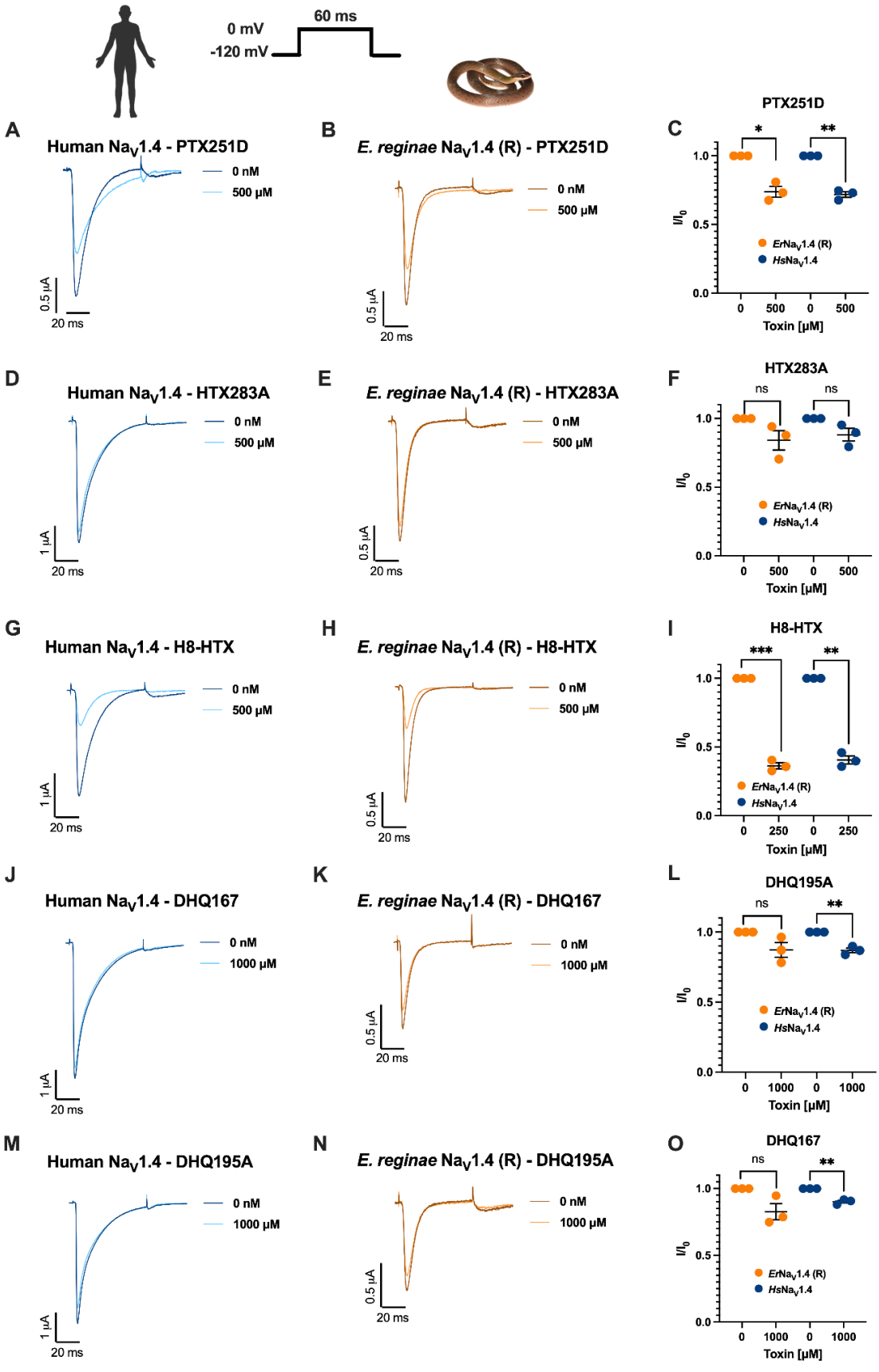
0 mV
-120 mV
60 ms
A
Human Na$_V$1.4 - PTX251D
0 nM
500 µM
0.5 µA
20 ms
B
E. reginae Na$_V$1.4 (R) - PTX251D
0 nM
500 µM
0.5 µA
20 ms
C
PTX251D
*
**
I/I$_0$
1.0
0.5
0.0
ErNa$_V$1.4 (R)
HsNa$_V$1.4
0
500
0
500
Toxin [µM]
D
Human Na$_V$1.4 - HTX283A
0 nM
500 µM
1 µA
20 ms
E
E. reginae Na$_V$1.4 (R) - HTX283A
0 nM
500 µM
0.5 µA
20 ms
F
HTX283A
ns
ns
I/I$_0$
1.0
0.5
0.0
ErNa$_V$1.4 (R)
HsNa$_V$1.4
0
500
0
500
Toxin [µM]
G
Human Na$_V$1.4 - H8-HTX
0 nM
500 µM
1 µA
20 ms
H
E. reginae Na$_V$1.4 (R) - H8-HTX
0 nM
500 µM
0.5 µA
20 ms
I
H8-HTX
***
**
I/I$_0$
1.0
0.5
0.0
ErNa$_V$1.4 (R)
HsNa$_V$1.4
0
250
0
250
Toxin [µM]
J
Human Na$_V$1.4 - DHQ167
0 nM
1000 µM
1 µA
20 ms
K
E. reginae Na$_V$1.4 (R) - DHQ167
0 nM
1000 µM
0.5 µA
20 ms
L
DHQ195A
ns
**
I/I$_0$
1.0
0.5
0.0
ErNa$_V$1.4 (R)
HsNa$_V$1.4
0
1000
0
1000
Toxin [µM]
M
Human Na$_V$1.4 - DHQ195A
0 nM
1000 µM
1 µA
20 ms
N
E. reginae Na$_V$1.4 (R) - DHQ195A
0 nM
1000 µM
0.5 µA
20 ms
O
DHQ167
ns
**
I/I$_0$
1.0
0.5
0.0
ErNa$_V$1.4 (R)
HsNa$_V$1.4
0
1000
0
1000
Toxin [µM]

Figure S7. *E. reginae* $Na_V1.4$ resistant variant is sensitive to other toxins found in dendrobatid frogs (B, E, H, K, N). Exemplar current recordings for Human $Na_V1.4$ (*Hs*$Na_V1.4$ in blue), and *E. reginae* $Na_V1.4$ resistant variant (*Er*$Na_V1.4$-R in orange) expressed in oocytes cells and exposed to (+)-pumiliotoxin 251D (PTX251D), histrionicotoxin 283A (HTX283A), (+/-)-H8-histrionicotoxin (H8-HTX), decahydroquinoline 167 (DHQ167), and decahydroquinoline 195A (DHQ195A). Comparison of sodium current reduction in the presence or absence of 500 μM PTX251D (**C**), 500 μM HTX283A (**F**), 500 μM H8-HTX (**I**), 1000 μM DHQ167 (**L**), and 1000 μM DHQ195A (**O**). Statistical significance was assessed using a one-sided T-test, with p-values provided for the corresponding comparisons. P-values are shown in the graph as (ns) $P > 0.01$; (*) $P \leq 0.01$; (**) $P \leq 0.01$; (***) $P \leq 0.001$.

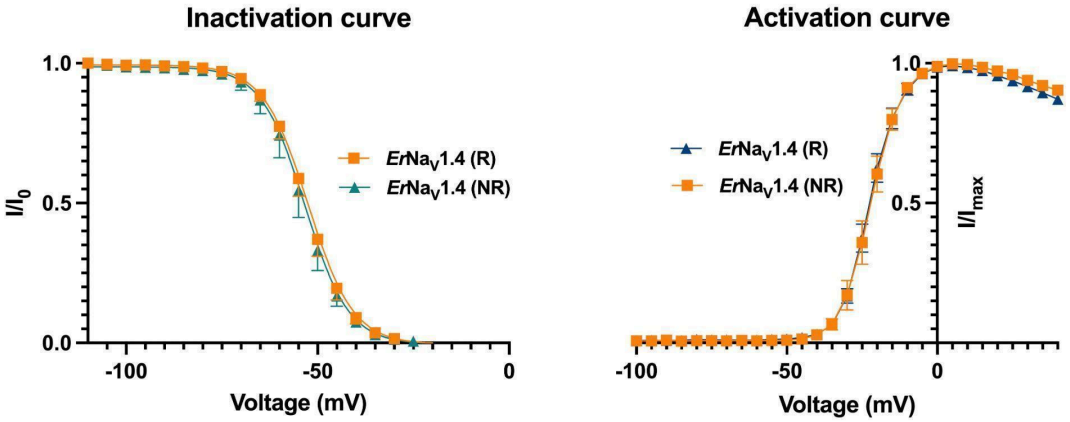

Figure S8. Inactivation and activation curve for the *E. reginae* $Na_V1.4$ "resistant" (R) and "non-resistant" (NR).

Toxin	Molecular weight	Weight (mg)	Diluted in
DHQ **195A** - PTX-C	231.80524	3.8	ddH2O
DHQ **167** (PTX-CIV, HCL salt)	203.75208	3.8	ddH2O
(+)-PTX **251D** (HCL salt)	287.8685	1.8	ddH2O
(+/-)-H8-HTX (HCL salt)	327.93236	2	ddH2O
Histrionicotoxin HTX **283A**	283.4079	2	ddH2O + 5%DMSO

Table S1. Stock and dilution details for toxins PTX **251D**, HTX **283A**, H8-HTX, DHQ **167**, and DHQ **195A**.

Toxin	*Hs*Na_V1.4	*Er*Na_V1.4-NR	*Er*Na_V1.4-R
TTX-TEVC			
IC50 (nM)	103.6 ± 28.32	18.09 ± 2.02	>>3000 nM
n	5	6	6
STX-TEVC			
IC50 (nM)	15.56 ± 4.217	6.565 ± 1.013	>>3000 nM
n	6	4	6
NeoSTX-TEVC			
IC50 (nM)	2.355 ± 1.170	0.4048 ± 0.235	>> 333 nM
n	6	6	6

Table S2. IC_{50} values for TTX, STX, and neoSTX for *Er*Na_V1.4-R "resistant" and *Er*Na_V1.4-NR "non-resistant" variants, and human Na_V1.4.

Essay	***Er*Na$_V$1.4 (NR)**	***Er*Na$_V$1.4 (R)**
Inactivation		
V50 (mV)	-53.32 ± 3.229	-52.47 ± 2.929
K (slope)	-5.712	-5.887
K (95% CI)	-6.116 to -5.326	-6.190 to -5.592
n	12	16
Activation		
V50 (mV)	-22.98 ± 3.382	-23.52 ± 3.554
K (slope)	4.21	3.939
K (95% CI)	3.647 to 4.810	3.508 to 4.392
n	6	14

Table S3. Inactivation and activation V_{50} and slope (K) values for *E. reginae* Na$_V$1.4-R "resistant" and *E. reginae* Na$_V$1.4-NR "non-resistant" variants, and human Na$_V$1.4.

Movie S1. Recording of *E. reginae* feeding on *S. ruber*. Field sample number VRC19.
Movie S2. Recording extract of dragging behavior of *E. reginae* feeding on *A. trivittata*. Field sample number VRC101.

Dataset S1. (separate file) *E. reginae* NCBI annotation of upregulated genes across four tissues (tongue, liver, stomach, and intestine) under three dietary conditions: consumption of *A. trivittata*, *S. ruber*, or fasting. Available in dryad (DOI: 10.5061/dryad.wstqjq302).
Dataset S2.1. (separate file) pcDNA3.1+ expression vectors containing the *E. reginae* $Na_v1.4$ "non-resistant" (NR) $Na_v1.4$ coding sequence. Available in dryad (DOI: 10.5061/dryad.wstqjq302).
Dataset S2.2. (separate file) pcDNA3.1+ expression vectors containing the human $Na_v1.4$ coding sequence. Available in dryad (DOI: 10.5061/dryad.wstqjq302).
Dataset S2.3. (separate file) pcDNA3.1+ expression vectors containing the *E. reginae* $Na_v1.4$ "resistant" (R) $Na_v1.4$ coding sequence. Available in dryad (DOI: 10.5061/dryad.wstqjq302).
Dataset S3.1. (separate file) Domain IV sequences of the *E. reginae* $Na_v1.4$ channel from field samples VRC09, used in the liver extract screening assay for functional toxin neutralization. Available in dryad (DOI: 10.5061/dryad.wstqjq302).
Dataset S3.2. (separate file) Domain IV sequences of the *E. reginae* $Na_v1.4$ channel from field samples VRC09, used in the liver extract screening assay for functional toxin neutralization. Available in dryad (DOI: 10.5061/dryad.wstqjq302).
Dataset S3.3. (separate file) Domain IV sequences of the *E. reginae* $Na_v1.4$ channel from field samples VRC10, used in the liver extract screening assay for functional toxin neutralization. Available in dryad (DOI: 10.5061/dryad.wstqjq302).
Dataset S3.4. (separate file) Domain IV sequences of the *E. reginae* $Na_v1.4$ channel from field samples VRC10, used in the liver extract screening assay for functional toxin neutralization. Available in dryad (DOI: 10.5061/dryad.wstqjq302).
Dataset S4. (separate file) Available predation experiments raw recordings. Available in dryad (DOI: 10.5061/dryad.wstqjq302).
Dataset S5. (separate file) Complete manuscript in Spanish. The Spanish translation was produced using ChatGPT and edited by VRC *(98)* (to be uploaded after revision). Available in dryad (DOI: 10.5061/dryad.wstqjq302).
Dataset S6. (separate file). General information and descriptions of the samples used in experimental assays, including museum specimen accession numbers and collection data. Available in dryad (DOI: 10.5061/dryad.wstqjq302).
Dataset S7. (separate file). Samples used for transcriptome analysis, including RIN values, SRA accession numbers, experimental condition, and tissue type. Available in dryad (DOI: 10.5061/dryad.wstqjq302).
Dataset S8. (separate file). List of genes annotated as transporters in the *E. reginae* NCBI genome annotation. Available in dryad (DOI: 10.5061/dryad.wstqjq302).

SI References

1. M. I. Love, W. Huber, S. Anders, Moderated estimation of fold change and dispersion for RNA-seq data with DESeq2. *Genome Biol.* **15**, 550 (2014).

2. A. Alexa, J. Rahnenfuhrer, *topGO: Enrichment Analysis for Gene Ontology* (2022).